Published for SISSA by Springer

Received: October 5, 2015
Accepted: February 3, 2016
Published: March 14, 2016

Measurement of D_s^+ production and nuclear modification factor in Pb-Pb collisions at $\sqrt{s_{NN}} = 2.76$ TeV

The ALICE collaboration

E-mail: ALICE-publications@cern.ch

Abstract: The production of prompt D_s^+ mesons was measured for the first time in collisions of heavy nuclei with the ALICE detector at the LHC. The analysis was performed on a data sample of Pb-Pb collisions at a centre-of-mass energy per nucleon pair, $\sqrt{s_{NN}}$, of 2.76 TeV in two different centrality classes, namely 0–10% and 20–50%. D_s^+ mesons and their antiparticles were reconstructed at mid-rapidity from their hadronic decay channel $D_s^+ \to \phi\pi^+$, with $\phi \to K^-K^+$, in the transverse momentum intervals $4 < p_T < 12\,\mathrm{GeV}/c$ and $6 < p_T < 12\,\mathrm{GeV}/c$ for the 0–10% and 20–50% centrality classes, respectively. The nuclear modification factor R_{AA} was computed by comparing the p_T-differential production yields in Pb-Pb collisions to those in proton-proton (pp) collisions at the same energy. This pp reference was obtained using the cross section measured at $\sqrt{s} = 7$ TeV and scaled to $\sqrt{s} = 2.76$ TeV. The R_{AA} of D_s^+ mesons was compared to that of non-strange D mesons in the 10% most central Pb-Pb collisions. At high p_T ($8 < p_T < 12\,\mathrm{GeV}/c$) a suppression of the D_s^+-meson yield by a factor of about three, compatible within uncertainties with that of non-strange D mesons, is observed. At lower p_T ($4 < p_T < 8\,\mathrm{GeV}/c$) the values of the D_s^+-meson R_{AA} are larger than those of non-strange D mesons, although compatible within uncertainties. The production ratios D_s^+/D^0 and D_s^+/D^+ were also measured in Pb-Pb collisions and compared to their values in proton-proton collisions.

Keywords: Hadron-Hadron scattering, Heavy ion Experiments, Quark gluon plasma

ArXiv ePrint: 1509.07287v1

doi:10.1007/JHEP03(2016)082

Contents

1 Introduction 1

2 Apparatus and data sample 4

3 $\mathrm{D_s^+}$ meson reconstruction and selection 5

4 Corrections 8

5 Systematic uncertainties 11

6 Results 15

7 Summary 19

The ALICE collaboration 26

JHEP03(2016)082

1 Introduction

Calculations of Quantum Chromodynamics (QCD) on the lattice predict that strongly-interacting matter at temperatures exceeding the pseudo-critical value of about $T_c \approx 145$–$165\,\mathrm{MeV}$ and vanishing baryon density behaves as a deconfined Plasma of Quarks and Gluons (QGP) [1, 2]. In this state, partons are the relevant degrees of freedom and chiral symmetry is predicted to be restored. The conditions to create a QGP are expected to be attained in collisions of heavy nuclei at high energies. This deconfined state of matter exists for a short time (few fm/c), during which the medium created in the collision expands and cools down until its temperature drops below the pseudo-critical value T_c and the process of hadronisation takes place.

Heavy quarks (charm and beauty) are sensitive probes to investigate the properties of the medium formed in heavy-ion collisions. They are produced in quark-antiquark pairs predominantly at the initial stage of the collision in hard-scattering processes characterized by timescales shorter than the QGP formation time [3–5]. The heavy quarks propagate through the expanding hot and dense medium, thus experiencing the effects of the medium over its entire evolution. While traversing the medium, they interact with its constituents via both inelastic and elastic QCD processes, exchanging energy and momentum with the expanding medium [5, 6]. For heavy quarks at intermediate and high momentum, these interactions lead to energy loss due to medium-induced gluon radiation and collisional processes.

Evidence for heavy-quark in-medium energy loss is provided by the observation of a substantial modification of the transverse momentum (p_{T}) distributions of heavy-flavour

decay leptons [7–10], D mesons [11, 12] and non-prompt J/ψ [13] in Au-Au and Pb-Pb collisions at RHIC and LHC energies as compared to proton-proton (pp) collisions. This modification is usually quantified by the nuclear modification factor $R_{\rm AA}$, defined as the ratio between the yield measured in nucleus-nucleus collisions and the cross section in pp interactions scaled by the average nuclear overlap function. In absence of nuclear effects, $R_{\rm AA}$ is expected to be unity. Parton in-medium energy loss causes a suppression of hadron yields, $R_{\rm AA} < 1$, at intermediate and high transverse momentum ($p_{\rm T} > 3\,{\rm GeV}/c$). In central nucleus-nucleus collisions at RHIC and LHC energies, $R_{\rm AA}$ values significantly lower than unity were observed for heavy-flavour hadrons with $p_{\rm T}$ values larger than 3–4 GeV/c. In this $p_{\rm T}$ range, the D-meson yields measured in p-Pb collisions at $\sqrt{s_{\rm NN}} = 5.02\,{\rm TeV}$ are consistent with binary-scaled pp cross sections [14], providing clear evidence that the suppression observed in Pb-Pb collisions is not due to cold nuclear matter effects and is induced by a strong coupling of the charm quarks with the hot and dense medium.

In case of substantial interactions with the medium, heavy quarks lose a significant amount of energy while traversing the fireball and may participate in the collective expansion of the system and possibly reach thermal equilibrium with the medium constituents. In this respect, the measurement of a positive elliptic flow v_2 of D mesons at LHC energies [15, 16] and of heavy-flavour decay electrons at RHIC energies [8, 9, 17] provides an indication that the interactions with the medium constituents transfer to charm quarks information on the azimuthal anisotropy of the system.

It is also predicted that a significant fraction of low- and intermediate-momentum heavy quarks could hadronise via recombination with other quarks from the medium [18–20]. An important role of hadronisation via (re)combination, either during the deconfined phase [21] or at the phase boundary [22], is indeed supported by the results of J/ψ nuclear modification factor and elliptic flow at low $p_{\rm T}$ [23–25]. Hadronisation via recombination allows in some models, e.g. [26–28], a better description of heavy-flavour production measurements at RHIC and LHC energies, in particular the $R_{\rm AA}$ of $\rm D^0$ mesons at low $p_{\rm T}$ measured in Au-Au collisions at $\sqrt{s_{\rm NN}} = 200\,{\rm GeV}$ [12] and the positive and sizable D-meson v_2 in Pb-Pb collisions at $\sqrt{s_{\rm NN}} = 2.76\,{\rm TeV}$ [15].

The measurement of $\rm D_s^+$-meson production in Pb-Pb collisions can provide crucial additional information for understanding the interactions of charm quarks with the strongly-interacting medium formed in heavy-ion collisions at high energies. In particular, the $\rm D_s^+$-meson yield is sensitive to strangeness production and to the hadronisation mechanism of charm quarks.

An enhancement of strange particle production in heavy-ion collisions as compared to pp interactions was long suggested as a possible signal of QGP formation [29, 30]. Strange quarks are expected to be abundant in a deconfined medium due to the short time needed to reach equilibrium values among the parton species and to the lower energy threshold for $s\bar{s}$ production. A pattern of strangeness enhancement increasing with the hadron strangeness content when going from pp (p-A) to heavy-ion collisions was observed at the SPS [31–34], at RHIC [35] and at the LHC [36]. In the frame of the statistical hadronisation models, strange particle production in heavy-ion collisions follows the expectation for a grand-canonical ensemble. In contrast, for pp collisions canonical suppression effects are

JHEP03(2016)082

found to be important, reducing the phase space available for strange particles [37, 38]. In this context, the increase in strange particle yields in heavy-ion collisions compared to pp interactions is viewed as due primarily to the lifting of the canonical suppression.

This strangeness enhancement effect could also affect the production of charmed hadrons if the dominant mechanism for D-meson formation at low and intermediate momenta is in-medium hadronisation of charm quarks via recombination with light quarks. Under these conditions, the relative yield of $\mathrm{D_s^+}$ mesons with respect to non-strange charmed mesons at low p_{T} is predicted to be enhanced in nucleus-nucleus collisions as compared to pp interactions [39–41]. The comparison of the p_{T}-differential production yields of non-strange D mesons and of $\mathrm{D_s^+}$ mesons in Pb-Pb and pp collisions is therefore sensitive to the role of recombination in charm-quark hadronisation.

A consequence of the possibly enhanced production of $\mathrm{D_s^+}$ mesons in heavy-ion collisions would be a slight reduction of the fraction of charm quarks hadronising into non-strange meson species. Therefore, the measurement of the $\mathrm{D_s^+}$-meson production is also relevant for the interpretation of the comparison of the nuclear modification factors of non-strange D mesons and light-flavour hadrons (pions) [11, 42], which is predicted to be sensitive to the quark-mass and colour-charge dependence of parton in-medium energy loss [6, 43, 44]. Furthermore, due to this possible modification of the relative abundances of D-meson species, measuring the $\mathrm{D_s^+}$ yield at low p_{T} is needed also to determine the total charm production cross section in Pb-Pb collisions.

The p_{T}-differential inclusive production cross section of prompt[1] $\mathrm{D_s^+}$ mesons (average of particles and antiparticles) was measured in pp collisions at $\sqrt{s} = 7\,\mathrm{TeV}$ with the ALICE detector and it was found to be described within uncertainties by perturbative QCD (pQCD) calculations [45]. The $\mathrm{D_s^+}$ nuclear modification factor was measured in p-Pb collisions at $\sqrt{s_{\mathrm{NN}}} = 5.02\,\mathrm{TeV}$ and found to be consistent with unity [14]. In this paper, we report on the measurement of prompt $\mathrm{D_s^+}$-meson production and nuclear modification factor in Pb-Pb collisions at $\sqrt{s_{\mathrm{NN}}} = 2.76\,\mathrm{TeV}$. $\mathrm{D_s^+}$ mesons (and their antiparticles) were reconstructed at mid-rapidity, $|y| < 0.5$, through their hadronic decay channel $\mathrm{D_s^+} \to \phi\pi^+$ with a subsequent decay $\phi \to \mathrm{K^-K^+}$. The production yield was measured in two classes of collision centrality, central (0–10%) and semi-central (20–50%), and compared to a binary-scaled pp reference obtained by scaling the cross section measured at $\sqrt{s} = 7\,\mathrm{TeV}$ to the Pb-Pb centre-of-mass energy via a pQCD-driven approach. The experimental apparatus and the data sample of Pb-Pb collisions used for this analysis are briefly presented in section 2. In section 3, the $\mathrm{D_s^+}$ meson reconstruction strategy, the selection criteria and the raw yield extraction from the $\mathrm{KK}\pi$ invariant mass distributions are discussed. The corrections applied to obtain the p_{T}-differential production yields of $\mathrm{D_s^+}$ mesons, including the subtraction of the non-prompt contribution from beauty-hadron decays, are described in section 4. The various sources of systematic uncertainty are discussed in detail in section 5. The results on the $\mathrm{D_s^+}$-meson production yield and nuclear modification factor

[1] In this paper, 'prompt' indicates D mesons produced at the interaction point, either directly in the hadronisation of the charm quark or in strong decays of excited charm resonances. The contribution from weak decays of beauty hadrons, which gives rise to feed-down D mesons displaced from the interaction vertex, was subtracted.

JHEP03(2016)082

are presented in section 6 together with the comparison to non-strange D-meson $R_{\rm AA}$ and to model calculations. The $\rm D_s^+/D^0$ and $\rm D_s^+/D^+$ yield ratios in three $p_{\rm T}$ intervals for the 10% most central Pb-Pb collisions are compared to those in pp collisions.

2 Apparatus and data sample

The ALICE detector and its performance are described in detail in refs. [46] and [47], respectively. The apparatus consists of a central barrel covering the pseudorapidity region $|\eta| < 0.9$, a forward muon spectrometer ($-4.0 < \eta < -2.5$) and a set of detectors for triggering and event centrality determination. The detectors of the central barrel are located inside a 0.5 T magnetic field parallel to the LHC beam direction, that corresponds to the z-axis in the ALICE reference frame. The information provided by the following detectors was utilised to perform the analysis presented in this paper: the Inner Tracking System (ITS), the Time Projection Chamber (TPC) and the Time Of Flight (TOF) detector were used to reconstruct and identify charged particles at mid-rapidity, while the V0 scintillator detector provided the information for triggering, centrality determination and event selection. The neutron Zero Degree Calorimeters (ZDC) were also used, together with the V0 detector, for the event selection.

The trajectories of the D-meson decay particles are reconstructed from their hits in the ITS and TPC detectors. Particle identification is performed utilising the information from the TPC and TOF detectors. The ITS consists of six cylindrical layers of silicon detectors covering the pseudorapidity interval $|\eta| < 0.9$. The two innermost layers, located at 3.9 and 7.6 cm from the beam line, are composed of Silicon Pixel Detectors (SPD). The two intermediate layers are equipped with Silicon Drift Detectors (SDD) and the two outermost layers, with a maximum radius of 43.0 cm, are composed of double-sided Silicon Strip Detectors (SSD). The high spatial resolution of the ITS detectors, together with the low material budget ($\sim 7.7\%$ of a radiation length at $\eta = 0$) and the small distance from the interaction point, provides a resolution on the track impact parameter (i.e. the distance of closest approach of the track to the primary vertex) better than 65 μm for transverse momenta $p_{\rm T} > 1\,{\rm GeV}/c$ in Pb-Pb collisions [47]. The TPC, covering the pseudorapidity interval $|\eta| < 0.9$, provides track reconstruction with up to 159 points along the trajectory of a charged particle and allows its identification via the measurement of specific energy loss $\mathrm{d}E/\mathrm{d}x$. Particle identification is complemented with the particle time-of-flight measured with the TOF detector, which is composed of Multi-gap Resistive Plate Chambers and is positioned at 370–399 cm from the beam axis, covering the full azimuth and the pseudorapidity interval $|\eta| < 0.9$. The TPC and TOF information provides pion/kaon separation at better than $3\,\sigma$ level for tracks with momentum up to $2.5\,{\rm GeV}/c$ [47].

The analysis was performed on a sample of Pb-Pb collisions at centre-of-mass energy per nucleon pair, $\sqrt{s_{\rm NN}}$, of 2.76 TeV collected in 2011. The events were recorded with an interaction trigger that required coincident signals in both scintillator arrays of the V0 detector, covering the pseudorapidity ranges $-3.7 < \eta < -1.7$ and $2.8 < \eta < 5.1$, respectively. An online selection based on the V0 signal amplitude was used to record samples of central and semi-central collisions through two separate trigger classes. Events

JHEP03(2016)082

Centrality class	$\langle T_{\rm AA} \rangle$ (mb^{-1})	$N_{\rm evt}$	$L_{\rm int}$ (μb^{-1})
0–10%	23.44 ± 0.76	16.4×10^6	21.3±0.7
20–50%	5.46 ± 0.20	13.5×10^6	5.8±0.2

Table 1. Average value of the nuclear overlap function, $\langle T_{\rm AA} \rangle$, for the considered centrality classes, expressed as percentiles of the hadronic Pb-Pb cross section. The values were obtained with a Monte Carlo implementation of the Glauber model assuming an inelastic nucleon-nucleon cross section of 64 mb [51]. The number of analysed events and the corresponding integrated luminosity in each centrality class are also shown. The uncertainty on the integrated luminosity derives from the uncertainty of the hadronic Pb-Pb cross section from the Glauber model [51].

were further selected offline to remove background from beam-gas interactions on the basis of the timing information provided by the V0 and the neutron ZDC detectors (two hadronic calorimeters located at $z = 114$ m on both sides of the interaction point covering the interval $|\eta| > 8.7$). Only events with an interaction vertex reconstructed from ITS+TPC tracks with $|z_{\rm vertex}| < 10$ cm were considered in the analysis.

Collisions were classified in centrality classes based on the sum of the signal amplitudes in the two V0 scintillator arrays. Each class is defined in terms of percentiles of the hadronic Pb-Pb cross section, as determined from a fit to the V0 signal amplitude distribution based on the Glauber-model description of the geometry of the nuclear collision [48–50] and a two-component model for particle production [51]. The analysis was performed in two centrality classes: 0–10% and 20–50%. In total, 16.5×10^6 events, corresponding to an integrated luminosity $L_{\rm int} = (21.5 \pm 0.7)$ μb^{-1}, were analysed in the 0–10% centrality class, and 13.5×10^6 events, $L_{\rm int} = (5.9 \pm 0.2)$ μb^{-1}, in the 20–50% class. The average values of the nuclear overlap function $T_{\rm AA}$ (defined as the convolution of the nuclear density profiles of the colliding ions [50] and proportional to the number $N_{\rm coll}$ of binary nucleon-nucleon collisions occurring in the Pb-Pb collision) are reported in table 1 for the 0–10% and 20–50% centrality classes, together with their systematic uncertainty estimated as described in [51].

3 $\mathrm{D_s^+}$ meson reconstruction and selection

$\mathrm{D_s^+}$ mesons and their antiparticles were reconstructed in the decay channel $\mathrm{D_s^+ \to \phi\pi^+ \to K^-K^+\pi^+}$ (and its charge conjugate), whose branching ratio (BR) is (2.24 ± 0.10)% [52]. Other $\mathrm{D_s^+}$ decay channels can give rise to the same $\mathrm{K^-K^+\pi^+}$ final state, such as $\mathrm{D_s^+ \to \overline{K}^{*0}K^+}$ and $\mathrm{D_s^+ \to f_0(980)\pi^+}$, with BR of (2.58 ± 0.11)% and (1.14 ± 0.31)%, respectively [52]. However, as explained in ref. [45], the applied cuts for the selection of the $\mathrm{D_s^+}$ signal candidates strongly reduce contributions from these channels, and therefore the measured yield is dominated by the $\mathrm{D_s^+ \to \phi\pi^+ \to K^-K^+\pi^+}$ decays. The decay channel through the ϕ resonance was chosen because the narrower width of the ϕ invariant-mass peak with respect to $\mathrm{f_0(980)}$ and $\mathrm{\overline{K}^{*0}}$ provides the best discrimination between signal and background.

JHEP03(2016)082

The analysis strategy for the extraction of the signal out of a large combinatorial background is based on the reconstruction of decay topologies with a secondary vertex significantly displaced from the interaction point. The secondary vertex position and its covariance matrix were determined from the decay tracks by using the same analytic χ^2 minimization method as for the computation of the primary vertex [53]. The resolution on the position of the $\mathrm{D_s^+}$ decay vertex was estimated with Monte Carlo simulations and it was found to be about 100 μm. $\mathrm{D_s^+}$ mesons have a mean proper decay length $c\tau = 150 \pm 2$ μm [52], which makes it possible to resolve their decay vertices from the primary vertex. With the current data sample, the signal of $\mathrm{D_s^+}$ mesons could be extracted in three p_{T} intervals (4–6, 6–8 and 8–12 GeV/c) in the 0–10% centrality class and in two p_{T} intervals (6–8 and 8–12 GeV/c) in the 20–50% centrality class.

$\mathrm{D_s^+}$ candidates were defined from triplets of tracks with the proper charge sign combination. Tracks were selected requiring $|\eta| < 0.8$ and $p_{\mathrm{T}} > 0.6$ (0.4) GeV/c in the 0–10% (20–50%) centrality class. In addition, tracks were also required to have at least 70 (out of a maximum of 159) associated hits in the TPC, a $\chi^2/\mathrm{ndf} < 2$ of the track momentum fit in the TPC and at least one associated hit in one of the two SPD layers. With these track selection criteria, the acceptance in rapidity for D mesons drops steeply to zero for $|y| \gtrsim 0.5$ at low p_{T} and for $|y| \gtrsim 0.8$ at $p_{\mathrm{T}} \gtrsim 5$ GeV/c. A p_{T}-dependent fiducial acceptance cut was therefore applied on the D-meson rapidity, $|y| < y_{\mathrm{fid}}(p_{\mathrm{T}})$, with $y_{\mathrm{fid}}(p_{\mathrm{T}})$ increasing from 0.5 to 0.8 in $0 < p_{\mathrm{T}} < 5$ GeV/c according to a second order polynomial function and taking a constant value of 0.8 for $p_{\mathrm{T}} > 5$ GeV/c.

$\mathrm{D_s^+}$ candidates were filtered by applying kinematical cuts and geometrical selections on the decay topology, together with particle identification criteria. The selection criteria were tuned in each p_{T} interval and centrality class to have a good statistical significance of the signal, while keeping the selection efficiency as high as possible. It was also checked that background fluctuations were not causing a distortion in the signal line shape by verifying that the $\mathrm{D_s^+}$-meson mass and its resolution were in agreement with the Particle Data Group (PDG) world-average value (1.969 GeV/c^2 [52]) and the Monte Carlo simulation results, respectively. The resulting selection criteria depend on the transverse momentum of the candidate and provide a selection efficiency that increases with increasing p_{T}.

The main variables used to select the $\mathrm{D_s^+}$ decay topology were the decay length (L), defined as the distance between the primary and secondary vertices, and the cosine of the pointing angle ($\cos\theta_{\mathrm{point}}$), which is the angle between the reconstructed $\mathrm{D_s^+}$ momentum and the line connecting the primary and secondary vertices. Additional selections were applied on the projections of decay length and cosine of pointing angle in the transverse plane xy (L_{xy}, $\cos\theta^{xy}_{\mathrm{point}}$), in order to exploit the better resolution on the track parameters in that plane. A further cut was applied on L_{xy} divided by its uncertainty ($L_{xy}/\sigma_{L_{xy}}$). The three tracks were also required to have a small distance to the reconstructed decay vertex, by defining the variable σ_{vertex} as the square root of the sum in quadrature of the distances of each track to the secondary vertex. To further suppress the combinatorial background, the angles $\theta^*(\pi)$, i.e. the angle between the pion in the KKπ rest frame and the KKπ flight line in the laboratory frame, and $\theta'(\mathrm{K})$, i.e. the angle between one of the kaons and the pion in the KK rest frame, were exploited. The cut values used for $\mathrm{D_s^+}$

JHEP03(2016)082

mesons with $4 < p_{\rm T} < 6\,{\rm GeV}/c$ in the 0–10% centrality class were: L, $L_{xy} > 500$ μm, $L_{xy}/\sigma_{L_{xy}} > 7.5$, $\cos\theta_{\rm point} > 0.94$, $\cos\theta^{xy}_{\rm point} > 0.94$, $\sigma_{\rm vertex} < 400$ μm, $\cos\theta^{*}(\pi) > 0.05$ and $|\cos^3\theta'({\rm K})| < 0.9$. Looser selection criteria were used for $\rm D_s^+$ selection at higher $p_{\rm T}$ and in more peripheral events, due to the lower combinatorial background.

In addition, to select $\rm D_s^+$ mesons decaying in the considered $\phi\pi^+$ mode, with $\phi \to {\rm K^-K^+}$, candidates were rejected if none of the two pairs of opposite-charged tracks had an invariant mass compatible with the PDG world average for the ϕ mass ($1.0195\,{\rm GeV}/c^2$ [52]). The difference between the reconstructed $\rm K^+K^-$ invariant mass and world-average ϕ mass was required to be less than $4\,{\rm MeV}/c^2$ (a selection that preserves about 70% of the signal) for $\rm D_s^+$ candidates in the three $p_{\rm T}$ intervals considered in the 0–10% centrality class, while looser selections were used for semi-central events.

Particle identification was used to obtain a further reduction of the background. Compatibility cuts were applied to the difference between the measured signals and those expected for a pion or a kaon. A track was considered compatible with the kaon or pion hypothesis if both its ${\rm d}E/{\rm d}x$ and time-of-flight were within $3\,\sigma$ from the expected values. Tracks without a TOF signal (mostly at low momentum) were identified using only the TPC information and requiring a $2\,\sigma$ compatibility with the expected ${\rm d}E/{\rm d}x$. Triplets of selected tracks were required to have two tracks compatible with the kaon hypothesis and one with the pion hypothesis. In addition, since the decay particle with opposite charge sign has to be a kaon, a triplet was rejected if the opposite-sign track was not compatible with the kaon hypothesis. This particle identification strategy preserves about 85% of the $\rm D_s^+$ signal.

For each candidate, two values of invariant mass can be computed, corresponding to the two possible assignments of the kaon and pion mass to the two same-sign tracks. Signal candidates with wrong mass assignment to the same-sign tracks would give rise to a contribution to the invariant-mass distributions that could potentially introduce a bias in the measured raw yield of $\rm D_s^+$ mesons. It was verified, both in data and in simulations, that this contribution is reduced to a negligible level by the particle identification selection and by the requirement that the invariant mass of the two tracks identified as kaons is compatible with the ϕ mass.

The invariant-mass distributions of the $\rm D_s^+$ candidates (sum of $\rm D_s^+$ and $\rm D_s^-$ candidates) are shown in figure 1 in the three $p_{\rm T}$ intervals for the 10% most central Pb-Pb collisions. The raw signal yields were extracted by fitting the invariant-mass distributions with a function that consists of the sum of a Gaussian term to describe the signal peak and an exponential function to describe the background. The fit was performed in the invariant-mass range $1.88 < M({\rm KK}\pi) < 2.1\,{\rm GeV}/c^2$ in all $p_{\rm T}$ intervals. The lower limit of $1.88\,{\rm GeV}/c^2$ was chosen to exclude the contribution of $\rm D^+ \to K^-K^+\pi^+$ decays, BR $= (0.265^{+0.008}_{-0.009})\%$ [52], which could give rise to a bump in the background shape for invariant-mass values around the $\rm D^+$ mass ($1.870\,{\rm GeV}/c^2$) [52]. The mean values of the Gaussian functions in all the $p_{\rm T}$ intervals are compatible within two times their uncertainty with the PDG world average for the $\rm D_s^+$ mass and the Gaussian widths are in agreement with the expected values from Monte Carlo simulations.

In table 2 the extracted raw yields of $\rm D_s^+$ mesons (sum of particle and antiparticle), defined as the integral of the Gaussian functions, are listed for the different $p_{\rm T}$ intervals

JHEP03(2016)082

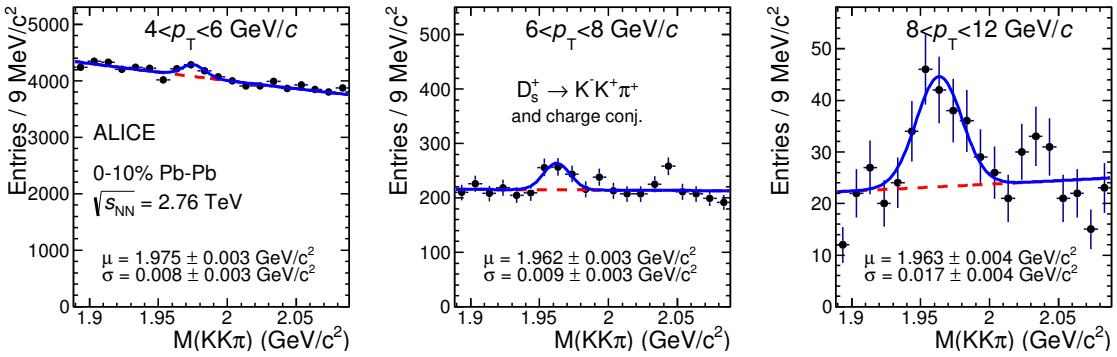

Figure 1. Invariant-mass distributions of $\mathrm{D_s^+}$ candidates and charge conjugates in the three considered p_{T} intervals in the 10% most central Pb-Pb collisions.

Centrality class	p_{T} interval (GeV/c)	$N^{\mathrm{D_s^\pm\ raw}}$	S/B (3σ)	S/$\sqrt{\mathrm{S+B}}$ (3σ)	χ^2/ndf
0–10%	4–6	438±144	0.02	3.0	27.4 / 18
	6–8	117± 38	0.10	3.2	17.5 / 18
	8–12	89± 21	0.38	5.0	26.5 / 18
20–50%	6–8	197± 61	0.07	3.5	9.9 / 21
	8–12	52± 20	0.29	3.4	17.9 / 21

Table 2. Measured raw yields ($N^{\mathrm{D_s^\pm\ raw}}$), signal over background (S/B), statistical significance (S/$\sqrt{\mathrm{S+B}}$) and χ^2/ndf of the invariant-mass fit for $\mathrm{D_s^+}$ and their antiparticles in the considered p_{T} intervals for the 0–10% and 20–50% centrality classes. The uncertainty on the $\mathrm{D_s^\pm}$ raw yield is the statistical uncertainty obtained from the fit.

in both the considered centrality classes, together with the signal-over-background (S/B) ratios and the statistical significance (S/$\sqrt{\mathrm{S+B}}$). The background was evaluated by integrating the background fit functions in $\pm 3\sigma$ around the centroid of the Gaussian.

4 Corrections

The raw yields extracted from the fits to the invariant-mass distributions of $\mathrm{D_s^+}$ and $\mathrm{D_s^-}$ candidates were corrected to obtain the production yields of prompt (i.e. not coming from weak decays of B mesons) $\mathrm{D_s^+}$ mesons. The p_{T}-differential yield of prompt $\mathrm{D_s^+}$ was computed as

$$\left.\frac{\mathrm{d}N^{\mathrm{D_s^+}}}{\mathrm{d}p_{\mathrm{T}}}\right|_{|y|<0.5} = \frac{1}{\Delta p_{\mathrm{T}}}\frac{1}{\mathrm{BR}\cdot N_{\mathrm{evt}}}\frac{f_{\mathrm{prompt}}(p_{\mathrm{T}})\cdot\frac{1}{2}N^{\mathrm{D_s^\pm\ raw}}(p_{\mathrm{T}})\Big|_{|y|<y_{\mathrm{fid}}}}{2y_{\mathrm{fid}}(p_{\mathrm{T}})\,(\mathrm{Acc}\times\epsilon)_{\mathrm{prompt}}(p_{\mathrm{T}})}\,, \tag{4.1}$$

where $N^{\mathrm{D_s^\pm\ raw}}(p_{\mathrm{T}})$ are the values of the raw yields (sum of particles and antiparticles) reported in table 2, which were corrected for the B-meson decay feed-down contribution

JHEP03(2016)082

(i.e. multiplied by the prompt fraction $f_{\rm prompt}$), divided by the acceptance-times-efficiency for prompt $\rm D_s^+$ mesons, $(\rm Acc \times \epsilon)_{\rm prompt}$, and divided by a factor of two to obtain the charge (particle and antiparticle) averaged yields. The corrected yields were divided by the decay channel branching ratio (BR), the $p_{\rm T}$ interval width ($\Delta p_{\rm T}$), the rapidity coverage ($2y_{\rm fid}$) and the number of analysed events ($N_{\rm evt}$).

The correction for the acceptance and the efficiency was determined using Monte Carlo simulations. Pb-Pb collisions at $\sqrt{s_{\rm NN}} = 2.76\,\rm TeV$ were simulated using the HIJING v1.383 event generator [54]. Prompt and feed-down $\rm D_s^+$ (and $\rm D_s^-$) signals were added with the PYTHIA v6.4.21 generator [55]. In order to minimize the bias on the detector occupancy, the number of D mesons injected into each HIJING event was adjusted according to the Pb-Pb collision centrality. The $p_{\rm T}$ distribution of the generated $\rm D_s^+$ mesons in the 0–10% centrality class was weighted in order to match the shape measured for $\rm D^0$ mesons in central Pb-Pb collisions [42]. For the 20–50% centrality class, the generated $p_{\rm T}$ distribution was defined based on FONLL perturbative QCD calculations [56, 57] multiplied by the nuclear modification factor predicted by the BAMPS partonic transport model [58], which reproduces the measured non-strange D-meson $R_{\rm AA}$ in semi-central collisions within uncertainties [16].

The generated particles were transported through the ALICE detector using the GEANT3 [59] particle transport package together with a detailed description of the geometry of the apparatus and of the detector response. The simulation was tuned to reproduce the position and width of the interaction vertex distribution, the number of active electronic channels and the accuracy of the detector calibration, and their time evolution within the Pb-Pb data taking period.

The efficiencies were evaluated in centrality classes corresponding to those used in the analysis of the data in terms of charged-particle multiplicity, hence of detector occupancy. In the left-hand panel of figure 2, the $(\rm Acc \times \epsilon)$ values for prompt and feed-down $\rm D_s^+$ mesons with rapidity $|y| < y_{\rm fid}$ are shown for the 0–10% centrality class. The same figure shows also the $(\rm Acc \times \epsilon)$ values for the case without the PID selections, demonstrating that this selection is about 85% efficient for the signal.

The magnitude of $(\rm Acc \times \epsilon)$ increases with increasing $p_{\rm T}$, from 0.4% in the lowest $p_{\rm T}$ interval up to 2% in $8 < p_{\rm T} < 12\,\rm GeV/\mathit{c}$. The $(\rm Acc \times \epsilon)$ values for $\rm D_s^+$ from beauty-hadron decays are larger than those for prompt $\rm D_s^+$ by a factor of approximately 2.5–3.5 depending on $p_{\rm T}$, because the decay vertices of the feed-down $\rm D_s^+$ mesons are more displaced from the primary vertex and they are, therefore, more efficiently selected by the analysis cuts. The efficiency of the selections used in the centrality interval 20–50% is higher by a factor of about two with respect to that in the most central events, because the smaller combinatorial background in semi-peripheral collisions allowed the usage of looser selections on the $\rm D_s^+$ candidates.

The ratio of prompt to inclusive contributions in the $\rm D_s^+$-meson raw yield, $f_{\rm prompt}$, was evaluated using a procedure similar to the one adopted for the pp measurement [45]. The contribution of feed-down from B decays in the raw yield depends on $p_{\rm T}$ and on the applied geometrical selection criteria. The feed-down contribution was estimated using the beauty-hadron production cross section from FONLL perturbative QCD calculations for

JHEP03(2016)082

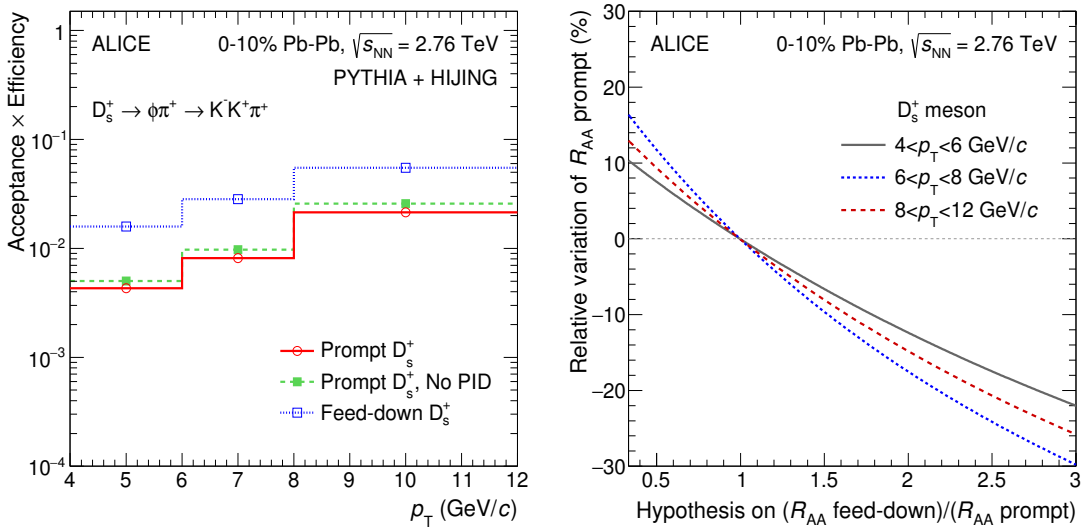

Figure 2. Left: acceptance-times-efficiency for D_s^+ mesons in the 10% most central Pb-Pb collisions. The efficiencies for prompt (solid lines) and feed-down (dotted lines) D_s^+ mesons are shown. Also displayed, for comparison, the efficiency for prompt D_s^+ mesons without PID selections (dashed lines). Right: relative variation of the prompt D_s^+-meson yield in the 0–10% centrality class as a function of the hypothesis on $R_{AA}^{\text{feed-down}}/R_{AA}^{\text{prompt}}$ for the B feed-down subtraction approach based on eq. (4.2).

pp collisions at $\sqrt{s} = 2.76\,\text{TeV}$ scaled by the average nuclear overlap function $\langle T_{AA}\rangle$ in each centrality class, the B→D+X decay kinematics from the EvtGen package [60] and the Monte Carlo efficiencies for feed-down D_s^+ mesons. The resulting sample of feed-down D_s^+ mesons is composed of two contributions: about 50% of the feed-down originates from B_s^0-meson decays, while the remaining 50% comes from decays of non-strange B mesons (B^0 and B^+). A hypothesis on the nuclear modification factor of feed-down D_s^+ mesons, $R_{AA}^{\text{feed-down}}$, was introduced to account for the different modification of beauty and charm production in Pb-Pb collisions and for the possible enhancement of the B_s^0 over non-strange B-meson yield due to the effect of hadronisation via recombination [61]. The fraction of prompt D_s^+ yield was therefore computed in each p_T interval as

$$\begin{aligned} f_{\text{prompt}} &= 1 - \frac{N^{D_s^+\ \text{feed-down raw}}}{N^{D_s^+\ \text{raw}}} \\ &= 1 - \langle T_{AA}\rangle \cdot \left(\frac{d^2\sigma}{dy dp_T}\right)^{\text{FONLL}}_{\text{feed-down}} \cdot R_{AA}^{\text{feed-down}} \cdot \frac{(\text{Acc}\times\epsilon)_{\text{feed-down}} \cdot 2y_{\text{fid}}\Delta p_T \cdot \text{BR} \cdot N_{\text{evt}}}{N^{D_s^\pm\ \text{raw}}/2}, \end{aligned} \tag{4.2}$$

where $(\text{Acc}\times\epsilon)_{\text{feed-down}}$ is the acceptance-times-efficiency for feed-down D_s^+ mesons. To determine the central value of f_{prompt}, it was assumed that the nuclear modification factors of feed-down and prompt D_s^+ mesons were equal ($R_{AA}^{\text{feed-down}} = R_{AA}^{\text{prompt}}$). The resulting feed-down contribution is about 20–25% depending on the p_T interval. To determine the systematic uncertainty the hypothesis was varied in the range $1/3 < R_{AA}^{\text{feed-down}}/R_{AA}^{\text{prompt}} < 3$, as discussed in detail in section 5. It should be noted that the central value and the

JHEP03(2016)082

range of the hypothesis on $R_{\rm AA}^{\rm feed\text{-}down}/R_{\rm AA}^{\rm prompt}$ differ from those used for non-strange D mesons in refs. [15, 16, 42], owing to the unknown role of recombination in the beauty sector, which could enhance the ratio of $\rm B_s^0$ over non-strange B mesons, and to the large fraction of feed-down $\rm D_s^+$ mesons originating from non-strange B-meson decays.

The nuclear modification factor of $\rm D_s^+$ mesons was computed as

$$R_{\rm AA}(p_{\rm T}) = \frac{{\rm d}N_{\rm AA}^{\rm D_s^+}/{\rm d}p_{\rm T}}{\langle T_{\rm AA}\rangle \, {\rm d}\sigma_{\rm pp}^{\rm D_s^+}/{\rm d}p_{\rm T}}. \tag{4.3}$$

The values of the average nuclear overlap function, $\langle T_{\rm AA}\rangle$, for the considered centrality classes are reported in table 1. The $p_{\rm T}$-differential cross section of prompt $\rm D_s^+$ mesons with $|y| < 0.5$ in pp collisions at $\sqrt{s} = 2.76\,\text{TeV}$, used as reference for $R_{\rm AA}$, was obtained by scaling in energy the measurement at $\sqrt{s} = 7\,\text{TeV}$ [45]. The ratio of the cross sections from FONLL pQCD calculations [57] at $\sqrt{s} = 2.76$ and $7\,\text{TeV}$ was used as the scaling factor. Since FONLL does not have a specific prediction for $\rm D_s^+$ mesons, the cross sections of the D-meson admixture (70% of $\rm D^0$ and 30% of $\rm D^+$) were used for the scaling. The theoretical uncertainty on the scaling factor was evaluated by considering the envelope of the results obtained by varying independently the factorisation and renormalisation scales and the charm quark mass, as explained in detail in ref. [62]. For $\rm D^0$, $\rm D^+$ and $\rm D^{*+}$ mesons, the result of the scaling was validated by comparison with data [63].

5 Systematic uncertainties

The systematic uncertainties on the prompt $\rm D_s^+$-meson yields in Pb-Pb collisions are summarised in table 3.

The systematic uncertainty on the raw-yield extraction was estimated from the distribution of the results obtained by repeating the fit to the invariant-mass spectra varying i) the fit range and ii) the probability distribution functions used to model the signal and background contributions. In particular, a second order polynomial function was used as an alternative functional form to describe the background. The signal line shape was varied by using Gaussian functions with mean and width fixed to the world-average $\rm D_s^+$ mass and to the values expected from Monte Carlo simulations, respectively. Furthermore, the raw yield was also extracted by counting the entries in the invariant-mass distributions after subtraction of the background estimated from a fit to the side bands of the $\rm D_s^+$ peak. In case of fitting in an extended mass range, it was verified that the effect on the $\rm D_s^+$ yield due to the possible bump produced in the candidate invariant-mass distribution by $\rm D^+ \to \phi\pi^+ \to K^-K^+\pi^+$ decays was negligible. An additional test was performed by fitting the $\rm D_s^+$ candidate invariant-mass distribution after subtracting the background estimated by coupling a pion track with $\rm K^+K^-$ pairs having an invariant mass in the side bands of the ϕ peak. The uncertainty was estimated to be 8% in all $p_{\rm T}$ intervals.

The contribution to the measured yield from $\rm D_s^+$ decaying into the $\rm K^-K^+\pi^+$ final state via other resonant channels (i.e. not via a ϕ meson) was found to be negligible, due to the much lower selection efficiency, as discussed in ref. [45].

JHEP03(2016)082

	0–10% centrality			20–50% centrality	
	p_{T} interval (GeV/c)			p_{T} interval (GeV/c)	
	4–6	6–8	8–12	6–8	8–12
Raw yield extraction	8%	8%	8%	8%	8%
Tracking efficiency	15%	15%	15%	15%	15%
Selection efficiency	20%	20%	20%	20%	20%
PID efficiency	7%	7%	7%	7%	7%
MC p_{T} shape	2%	1%	1%	1%	1%
Feed-down from B					
FONLL feed-down corr.	$^{+\ 6}_{-28}$%	$^{+10}_{-27}$%	$^{+\ 7}_{-27}$%	$^{+\ 6}_{-20}$%	$^{+\ 7}_{-25}$%
$R_{\mathrm{AA}}^{\text{feed-down}}/R_{\mathrm{AA}}^{\text{prompt}}$ (eq. (4.2))	$^{+10}_{-22}$%	$^{+16}_{-30}$%	$^{+13}_{-26}$%	$^{+11}_{-22}$%	$^{+12}_{-24}$%
Centrality limits	< 1%			< 1%	
Branching ratio	4.5%				

Table 3. Relative systematic uncertainties on p_{T}-differential yields of prompt $\mathrm{D_s^+}$ mesons in Pb-Pb collisions for the two considered centrality classes.

Other contributions to the systematic uncertainty originate from the imperfect implementation of the detector description in the Monte Carlo simulations, which could affect the particle reconstruction, the $\mathrm{D_s^+}$ selection efficiency, and the kaon and pion identification.

The systematic uncertainty on the tracking efficiency (including the effect of the track selection) was estimated by comparing the efficiency (i) of track finding in the TPC and (ii) of track prolongation from the TPC to the ITS between data and simulations, and (iii) by varying the track quality selections. The estimated uncertainty is 5% per track, which results in 15% for the three-body decay of $\mathrm{D_s^+}$ mesons.

The effect of residual discrepancies between data and simulations on the variables used to select the $\mathrm{D_s^+}$ candidates was estimated by repeating the analysis with different geometrical selections on the decay topology and varying the cut on the compatibility between the $\mathrm{K^+K^-}$ invariant mass and the ϕ mass. A systematic uncertainty of 20% was estimated from the spread of the resulting corrected yields.

The systematic uncertainty induced by a different efficiency for particle identification in data and simulations was estimated by comparing the corrected $\mathrm{D_s^+}$ yields obtained using different PID approaches, testing both looser and tighter cuts with respect to the baseline selection described in section 4. Due to the limited statistical significance, an analysis without PID selection could not be carried out. Such a test was performed in the analysis of $\mathrm{D^0}$ ($\to \mathrm{K^-}\pi^+$), $\mathrm{D^+}$ ($\to \mathrm{K^-}\pi^+\pi^+$) and $\mathrm{D^{*+}}$ ($\to \mathrm{D^0}\pi^+$) and a 5% uncertainty was estimated for the case of $3\,\sigma$ cuts on $\mathrm{d}E/\mathrm{d}x$ and time-of-flight signals, which correspond to the loosest selections that could be tested for the $\mathrm{D_s^+}$. Based on all these checks a systematic uncertainty of 7% on the PID selection efficiency was estimated.

JHEP03(2016)082

The efficiency is also sensitive to differences between the real and simulated $\mathrm{D_s^+}$ momentum distributions. The effect depends on the width of the p_{T} intervals and on the variation of the efficiency within them. A systematic uncertainty was defined from the relative difference among the efficiencies obtained using different p_{T} shapes for the generated $\mathrm{D_s^+}$ mesons, namely the measured $\mathrm{d}N/\mathrm{d}p_{\mathrm{T}}$ of $\mathrm{D^0}$ mesons in central Pb-Pb collisions, the p_{T} shape predicted by FONLL pQCD calculations with and without the nuclear modification predicted by the BAMPS partonic transport model. The resulting contribution to the systematic uncertainty was found to be 2% for the momentum interval $4 < p_{\mathrm{T}} < 6\,\mathrm{GeV}/c$, where the selection efficiency is strongly p_{T} dependent, and 1% at higher p_{T}.

The systematic uncertainty due to the subtraction of $\mathrm{D_s^+}$ mesons from B-meson decays was estimated following the procedure described in ref. [11]. The contribution of the uncertainties inherent in the FONLL perturbative calculation was included by varying the heavy-quark masses and the factorisation and renormalisation scales, μ_{F} and μ_{R}, independently in the ranges $0.5 < \mu_{\mathrm{F}}/m_{\mathrm{T}} < 2$, $0.5 < \mu_{\mathrm{R}}/m_{\mathrm{T}} < 2$, with the constraint $0.5 < \mu_{\mathrm{F}}/\mu_{\mathrm{R}} < 2$, where $m_{\mathrm{T}} = \sqrt{p_{\mathrm{T}}^2 + m_{\mathrm{Q}}^2}$. Furthermore, the prompt fraction obtained in each p_{T} interval was compared with the results of a different procedure in which the FONLL cross sections for prompt and feed-down D mesons and their respective Monte Carlo efficiencies were the input for evaluating the correction factor

$$f'_{\mathrm{prompt}} = \left(1 + \frac{(\mathrm{Acc} \times \epsilon)_{\text{feed-down}}}{(\mathrm{Acc} \times \epsilon)_{\mathrm{prompt}}} \cdot \frac{\left(\frac{\mathrm{d}^2\sigma}{\mathrm{d}y\,\mathrm{d}p_{\mathrm{T}}}\right)^{\mathsf{FONLL}}_{\text{feed-down}}}{\left(\frac{\mathrm{d}^2\sigma}{\mathrm{d}y\,\mathrm{d}p_{\mathrm{T}}}\right)^{\mathsf{FONLL}}_{\mathrm{prompt}}} \cdot \frac{R_{\mathrm{AA}}^{\text{feed-down}}}{R_{\mathrm{AA}}^{\mathrm{prompt}}} \right)^{-1} . \tag{5.1}$$

Since FONLL does not have a specific prediction for $\mathrm{D_s^+}$ mesons, four different approaches were used to compute the predicted p_{T} shapes of promptly produced $\mathrm{D_s^+}$, $\left(\mathrm{d}^2\sigma/\mathrm{d}y\,\mathrm{d}p_{\mathrm{T}}\right)^{\mathsf{FONLL}}_{\mathrm{prompt}}$, as explained in detail in ref. [45]: (i) FONLL prediction for the admixture of charm hadrons; (ii) FONLL prediction for $\mathrm{D^{*+}}$ mesons (the $\mathrm{D^{*+}}$ mass being close to that of the $\mathrm{D_s^+}$); (iii) FONLL prediction for c quarks and fragmentation functions from [64] with parameter $r = (m_{\mathrm{D}} - m_{\mathrm{c}})/m_{\mathrm{D}}$ (m_{D} and m_{c} being the masses of the considered D-meson species and of the c quark, respectively); (iv) FONLL prediction for c quarks and fragmentation functions from [64] with parameter $r = 0.1$ (as used in FONLL calculations) for all meson species. In the latter two cases, the $\mathrm{D_s^{*+}}$ mesons produced in the c quark fragmentation were made to decay with PYTHIA and the resulting $\mathrm{D_s^+}$ were summed to the primary ones to obtain the prompt yield. The systematic uncertainty due to the B feed-down subtraction was finally evaluated as the envelope of the results obtained with the two methods, namely eq. (4.2) and (5.1), when varying the FONLL parameters and the $\mathrm{c} \to \mathrm{D_s^+}$ fragmentation function used to determine $\left(\mathrm{d}^2\sigma/\mathrm{d}y\,\mathrm{d}p_{\mathrm{T}}\right)^{\mathsf{FONLL}}_{\mathrm{prompt}}$ in eq. (5.1).

The contribution due to the different nuclear modification factor of prompt and feed-down $\mathrm{D_s^+}$ mesons was estimated by varying the hypothesis on $R_{\mathrm{AA}}^{\text{feed-down}}/R_{\mathrm{AA}}^{\mathrm{prompt}}$ in the range $1/3 < R_{\mathrm{AA}}^{\text{feed-down}}/R_{\mathrm{AA}}^{\mathrm{prompt}} < 3$ for both feed-down subtraction methods. The variation of the hypothesis is motivated by the combined effect on the R_{AA} of (i) the different energy loss of charm and beauty quarks in the QGP, as predicted by energy loss models and supported by experimental data on D meson and non-prompt J/ψ R_{AA} at the LHC [11,

JHEP03(2016)082

	$p_{\rm T}$ interval (GeV/c)		
	4–6	6–8	8–12
Data systematics in pp	26%	25%	29%
Feed-down from B	$^{+\ 4}_{-17}$%	$^{+\ 6}_{-15}$%	$^{+\ 5}_{-17}$%
$\sqrt{s}$-scaling of the pp reference	$^{+14}_{-\ 7}$%	$^{+10}_{-\ 6}$%	$^{+\ 8}_{-\ 5}$%
Normalisation	3.5%		
Branching ratio	4.5%		

Table 4. Relative systematic uncertainties on the pp reference cross section. The row labeled 'Data systematics' reports the sum in quadrature of the contributions due to raw yield extraction, tracking efficiency, selection efficiency, PID efficiency, MC $p_{\rm T}$ shape and 'other resonant channels' from ref. [45].

13, 42, 65, 66]; (ii) the possibly different contribution of coalescence in charm and beauty quark hadronisation, leading to a different abundance of $\rm D_s^+$ and $\rm B_s^0$ mesons relative to non-strange mesons; and (iii) the possibly different modulation of D and B spectra due to radial flow. The resulting uncertainty for the case of B feed-down subtraction approach based on eq. (4.2) is shown in the right-hand panel of figure 2 for the three $p_{\rm T}$ intervals in the 0–10% centrality class.

The Pb-Pb data are also affected by a systematic uncertainty on the determination of the limits of the centrality classes, due to the 1.1% relative uncertainty on the fraction of the total hadronic cross section used in the Glauber fit [51]. This contribution was estimated from the variation of the D-meson $\rm d\mathit{N}/d\mathit{p}_T$ when the limits of the centrality classes are shifted by ±1.1%. The resulting uncertainty, which is common to all $p_{\rm T}$ bins, is less than 1% for both the 0–10% and the 20–50% centrality classes.

Finally, the 4.5% uncertainty on the branching ratio [52] was considered.

In the calculation of the $R_{\rm AA}$, the uncertainties on the reference cross section for pp collisions, the Pb-Pb yields, and the average nuclear overlap function were considered.

For the pp reference, the uncertainties on the measurement at $\sqrt{s} = 7\,\text{TeV}$, described in ref. [45] and those due to the FONLL-based scaling to $\sqrt{s} = 2.76\,\text{TeV}$, described in section 4, were summed in quadrature. The contributions to the systematic uncertainty on the pp reference cross section are reported in table 4.

The uncertainties on the pp reference were added in quadrature to those on the Pb-Pb prompt $\rm D_s^+$ yields, described above, except for the BR that cancels out in the ratio and the feed-down contribution deriving from FONLL uncertainties, that partly cancels in the ratio. This contribution was evaluated by comparing the $R_{\rm AA}$ values obtained with the two methods for feed-down correction of eq. (4.2) and (5.1) and with the different heavy-quark masses, fragmentation functions, factorisation and renormalisation scales used in FONLL. In this study, these variations were done simultaneously for the Pb-Pb yield and for the pp reference cross section, so as to take into account the correlations of these sources in the numerator and denominator of $R_{\rm AA}$.

Finally, the $R_{\rm AA}$ normalisation uncertainty was computed as the quadratic sum of the 3.5% pp normalisation uncertainty [45], the contribution due to the 1.1% uncertainty

JHEP03(2016)082

on the fraction of hadronic cross section used in the Glauber fit discussed above, and the uncertainty on $\langle T_{\rm AA}\rangle$, which is of 3.2% and 3.7% for the 0–10% and 20–50% centrality classes, respectively.

6 Results

The transverse momentum distributions $\mathrm{d}N/\mathrm{d}p_{\rm T}$ of prompt $\mathrm{D_s^+}$ mesons in Pb-Pb collisions are shown in figure 3, for the 0–10% and 20–50% centrality classes. The yields reported in figure 3 refer to particles only, since they were computed as the average of particles and antiparticles under the assumption that the production cross section is the same for $\mathrm{D_s^+}$ and $\mathrm{D_s^-}$. The vertical error bars represent the statistical uncertainties. The symbols are positioned horizontally at the centre of each $p_{\rm T}$ interval, with the horizontal bars representing the width of the $p_{\rm T}$ interval. The systematic uncertainties from data analysis are shown as empty boxes around the data points, while those due to the B feed-down subtraction, which include the contributions of the FONLL uncertainties and of the variation of the hypothesis on $R_{\rm AA}^{\text{feed-down}}/R_{\rm AA}^{\text{prompt}}$, are displayed as shaded boxes. The normalisation uncertainties are reported as text on the figures.

The $p_{\rm T}$-differential yields measured in Pb-Pb collisions are compared to the reference yields in pp collisions at the same energy, scaled by the nuclear overlap function $\langle T_{\rm AA}\rangle$, reported in table 1. The pp reference at $\sqrt{s} = 2.76\,\text{TeV}$ is obtained by scaling the cross section measured at 7 TeV as described in section 4. A clear suppression of the $\mathrm{D_s^+}$-meson yield in the 10% most central Pb-Pb collisions relative to the binary-scaled pp yields is observed in the highest $p_{\rm T}$ interval ($8 < p_{\rm T} < 12\,\text{GeV}/c$). In the 20–50% centrality class, an indication of suppression is found in $8 < p_{\rm T} < 12\,\text{GeV}/c$. At lower $p_{\rm T}$, in both centrality classes, it is not possible to conclude on the presence of a suppression of the $\mathrm{D_s^+}$-meson yield in heavy-ion collisions with respect to the pp reference.

The nuclear modification factor $R_{\rm AA}$ of prompt $\mathrm{D_s^+}$ mesons was computed from the $\mathrm{d}N/\mathrm{d}p_{\rm T}$ distributions. The results are shown as a function of $p_{\rm T}$ in the left-hand panel of figure 4 for the two centrality classes. The vertical bars represent the statistical uncertainties, the empty boxes are the total $p_{\rm T}$-dependent systematic uncertainties described in section 5, except for the normalisation uncertainty, which is displayed as a filled box at $R_{\rm AA} = 1$. A suppression by a factor of about three of the $\mathrm{D_s^+}$-meson yield in Pb-Pb collisions relative to the binary-scaled pp cross section is observed in the highest $p_{\rm T}$ interval ($8 < p_{\rm T} < 12\,\text{GeV}/c$) for the 10% most central collisions. A smaller suppression (by a factor of about two) is measured in the 20–50% centrality class in $8 < p_{\rm T} < 12\,\text{GeV}/c$, even though with the current uncertainties no conclusions can be drawn on the centrality dependence of the $\mathrm{D_s^+}$-meson nuclear modification factor at high $p_{\rm T}$. Since no significant modification of the $\mathrm{D_s^+}$-meson production relative to binary-scaled pp collisions is observed in p-Pb reactions in the $p_{\rm T}$ range considered here [14], the substantial suppression of the $\mathrm{D_s^+}$-meson yield at high $p_{\rm T}$ in Pb-Pb collisions cannot be explained in terms of initial state effects, but it is predominantly due to strong final-state effects induced by the hot and dense partonic medium created in the collisions of heavy nuclei. At lower $p_{\rm T}$ the central values of the measurement show a larger $R_{\rm AA}$, however the large statistical and systematic

JHEP03(2016)082

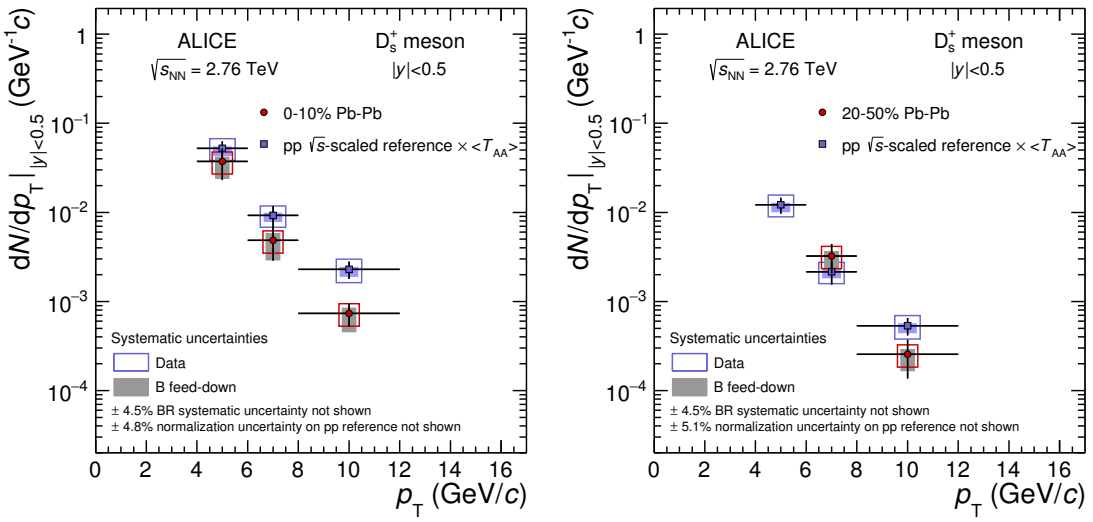

Figure 3. Transverse momentum distributions $\mathrm{d}N/\mathrm{d}p_\mathrm{T}$ of prompt $\mathrm{D_s^+}$ mesons in the 0–10% (left panel) and 20–50% (right panel) centrality classes in Pb-Pb collisions at $\sqrt{s_\mathrm{NN}} = 2.76\,\mathrm{TeV}$. Statistical uncertainties (bars), systematic uncertainties from data analysis (empty boxes) and systematic uncertainties due to beauty feed-down subtraction (shaded boxes) are shown. The reference pp distributions $\langle T_\mathrm{AA}\rangle\ \mathrm{d}\sigma/\mathrm{d}p_\mathrm{T}$ are shown as well.

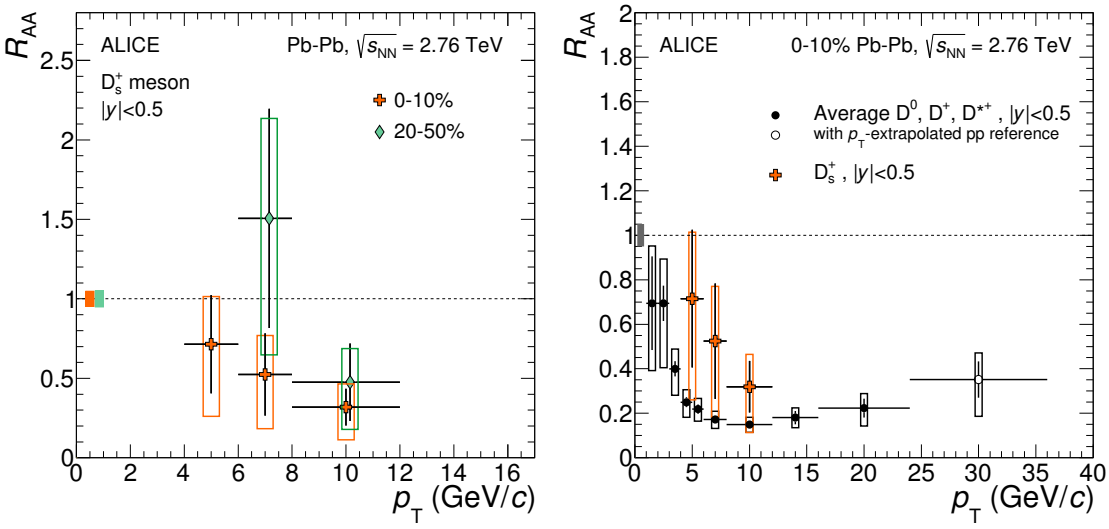

Figure 4. Left: R_AA of prompt $\mathrm{D_s^+}$ mesons in the 0–10% and 20–50% centrality classes as a function of p_T. For the 20–50% case, the symbols are displaced horizontally for visibility. Right: R_AA of prompt $\mathrm{D_s^+}$ mesons compared to non-strange D mesons (average of $\mathrm{D^0}$, $\mathrm{D^+}$ and $\mathrm{D^{*+}}$ [42]) in the 0–10% centrality class. Statistical (bars), systematic (empty boxes), and normalisation (full box) uncertainties are shown.

uncertainties do not allow to draw a conclusion on the p_T dependence of the $\mathrm{D_s^+}$ nuclear modification factor.

The R_AA of prompt $\mathrm{D_s^+}$ mesons in the 10% most central collisions is compared in the right-hand panel of figure 4 to the average nuclear modification factor of $\mathrm{D^0}$, $\mathrm{D^+}$ and $\mathrm{D^{*+}}$

JHEP03(2016)082

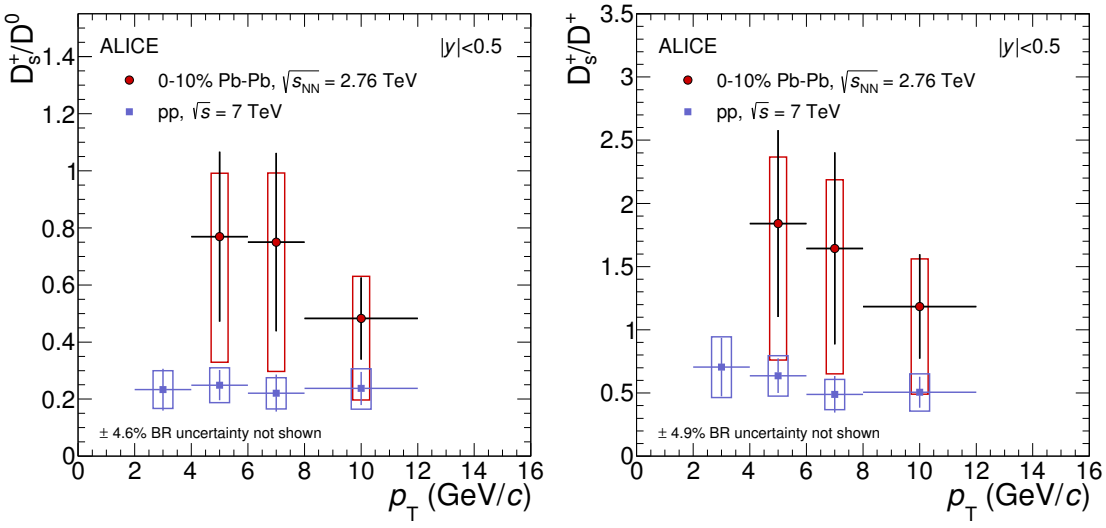

Figure 5. Ratios of prompt D-meson yields (D_s^+/D^0 and D_s^+/D^+) as a function of p_T in the 10% most central Pb-Pb collisions at $\sqrt{s_{NN}} = 2.76$ TeV compared to the results in pp collisions at $\sqrt{s} = 7$ TeV. Statistical (bars) and systematic (boxes) uncertainties are shown.

mesons measured in the same centrality class [42]. This comparison is meant to address the expected effect of hadronisation via quark recombination in the partonic medium on the relative abundances of strange and non-strange D-meson species. In the three p_T intervals, the values of the D_s^+-meson R_{AA} are higher than those of non-strange D mesons, although compatible within uncertainties. Even considering that a part of the systematic uncertainty is correlated between strange and non-strange D mesons, the current uncertainties do not allow a conclusive statement on the expected enhancement of the D_s^+-meson yield relative to that of non-strange D mesons in heavy-ion collisions.

An alternative approach to study the predicted modification of the charm-quark hadronisation in the presence of a QGP is to compare the ratios between the measured yields of D_s^+ and $D^0(D^+)$ mesons in Pb-Pb and pp collisions. This comparison is shown in figure 5 for the 10% most central Pb-Pb collisions. In the left-hand panel the D_s^+/D^0 ratio is displayed, while the right-hand panel shows the ratio D_s^+/D^+. The ratios D_s^+/D^0 and D_s^+/D^+ in pp collisions are taken from the measurements at $\sqrt{s} = 7$ TeV [45].[2] No strong dependence on the collision energy is expected (see [45] and references therein). In the evaluation of the systematic uncertainties on the D-meson yield ratios, the sources of correlated and uncorrelated systematic effects were treated separately. In particular, the contributions of the yield extraction, topological selection efficiency and PID efficiency were considered as uncorrelated and summed in quadrature. The uncertainty on the tracking efficiency cancels completely in the ratios between production cross sections of meson species reconstructed from three-body decay channels (D^+ and D_s^+), while a 5% systematic uncertainty (4% in

[2]The values from ref. [45] were re-computed with the most recent value for the branching ratio of the $D_s^+ \to \phi\pi^+ \to K^-K^+\pi^+$ decay chain, which is 2.24% [52], while it was 2.28% at the time of the pp publication.

JHEP03(2016)082

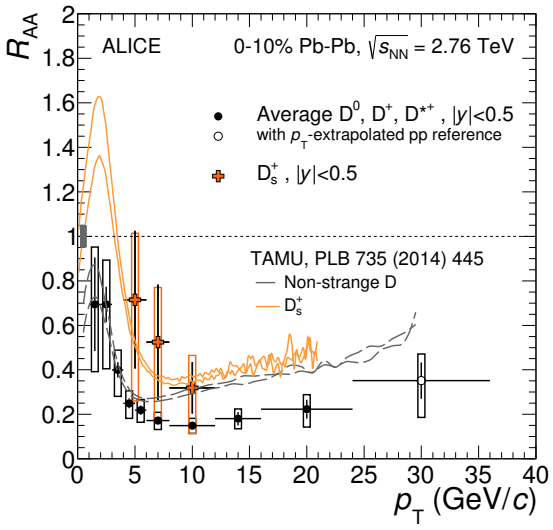

Figure 6. $R_{\rm AA}$ of prompt $\rm D_s^+$ and non-strange D mesons (average of $\rm D^0$, $\rm D^+$ and $\rm D^{*+}$) in the 0–10% centrality class compared to predictions of the TAMU model [61]. The bands shown for the TAMU predictions encompass the charm-shadowing uncertainty.

the pp case) was considered in the ratio to the $\rm D^0$ yields, which are reconstructed from a two-particle final state. To propagate the uncertainty due to the B feed-down subtraction, the contribution of the FONLL cross section was treated as completely correlated among the D-meson species. It was estimated from the spread of the D-meson yield ratios obtained by varying the factorisation and renormalisation scales and the heavy-quark mass in FONLL coherently for the three meson species. The contribution due to the hypothesis on $R_{\rm AA}^{\rm feed\text{-}down}/R_{\rm AA}^{\rm prompt}$ was considered as uncorrelated between $\rm D_s^+$ and non-strange D mesons and summed in quadrature. The difference between the $\rm D_s^+/D^0$ ratios in pp and in central Pb-Pb collisions is of about $1\,\sigma$ of the combined statistical and systematic uncertainties in both the two lowest $p_{\rm T}$ intervals, $4 < p_{\rm T} < 6\,{\rm GeV}/c$ and $6 < p_{\rm T} < 8\,{\rm GeV}/c$. An enhancement of $\rm D_s/D$ ratios in heavy-ion collisions is predicted if recombination contributes to charm quark hadronisation in the QGP. However, considering the current level of experimental uncertainties, no conclusion on charm-quark hadronisation can be drawn from this first measurement of $\rm D_s^+$-meson production in Pb-Pb collisions.

In the framework of the Statistical Hadronisation Model [39, 67, 68], the $p_{\rm T}$-integrated ratios of D-meson abundances for a chemical freeze-out temperature $T = 156\,{\rm MeV}$ (as extracted from fits to the measured abundances of light-flavour hadrons [69]) and vanishing baryo-chemical potential, are expected to be $\rm D_s^+/D^0 = 0.338$ and $\rm D_s^+/D^+ = 0.830$, which are higher by a factor of about two with respect to the values calculated for pp collisions at LHC energies [45].

In figure 6, the measured $R_{\rm AA}$ of non-strange D mesons and of $\rm D_s^+$ are compared to the prediction of the TAMU model [27, 61]. Among the several models available for open charm production in heavy-ion collisions, TAMU is the only one providing a quantitative prediction for the $\rm D_s^+$-meson nuclear modification factor. This is a heavy-quark transport model based on heavy-quark diffusion, implemented via simulations based on the relativis-

JHEP03(2016)082

tic Langevin equation, in a hydrodynamically expanding medium. The interactions of the charm quarks with the medium are modeled including only elastic processes, which are assumed to govern the heavy-quark scattering amplitudes at low and intermediate momenta. The heavy-quark transport coefficients are calculated within a non-perturbative T-matrix approach, where the interactions proceed via resonance formation that transfers momentum from the heavy quarks to the medium constituents. The hadronisation of charm quarks is performed via recombination with thermalized up, down and strange quarks. The remaining charm quarks are converted to hadrons using the vacuum fragmentation functions from [64] and fragmentation fractions $f(\mathrm{c} \to \mathrm{D})$ from PYTHIA. This model predicts an enhancement of the $\mathrm{D_s^+}$ over the non-strange D-meson R_{AA} at low p_{T} as a consequence of the recombination of charm quarks with thermally equilibrated strange quarks in the QGP. At higher p_{T}, where the dominant hadronisation mechanism is fragmentation, similar R_{AA} values are predicted for the different D-meson species. The model describes the measured $\mathrm{D_s^+}$-meson nuclear modification factor within uncertainties and at low p_{T} provides also a reasonable description of non-strange D-meson R_{AA}. The measured suppression of non-strange D mesons is underestimated at higher p_{T}, where the contribution of inelastic processes (gluon radiation), which are missing in this transport calculation, is expected to play a major role.

7 Summary

The production of $\mathrm{D_s^+}$ mesons was measured for the first time in heavy-ion collisions. The measurement was carried out on a sample of Pb-Pb collisions at $\sqrt{s_{\mathrm{NN}}} = 2.76\,\mathrm{TeV}$ in two centrality classes, namely 0–10% and 20–50%.

The results for the 10% most central collisions indicate a substantial suppression ($R_{\mathrm{AA}} \approx 0.3$) of the production of $\mathrm{D_s^+}$ mesons at high p_{T} ($8 < p_{\mathrm{T}} < 12\,\mathrm{GeV}/c$) with respect to the expectation based on the pp cross section scaled by the average nuclear overlap function. The observed suppression is compatible with that of non-strange D mesons and can be described by models including strong coupling of the charm quarks with the deconfined medium formed in the collision.

At lower momenta ($4 < p_{\mathrm{T}} < 8\,\mathrm{GeV}/c$), the values of the $\mathrm{D_s^+}$-meson nuclear modification factor are larger than those of non-strange D mesons, although compatible within uncertainties. This result provides a possible hint for an enhancement of $\mathrm{D_s/D}$ ratio, which is expected if the recombination process significantly contributes to the charm quark hadronisation in the QGP.

The precision of the measurements will be improved using the larger data samples of Pb-Pb collisions that will be collected during the ongoing LHC Run-2. The larger sample size will allow us to observe the $\mathrm{D_s^+}$ signal with less stringent selections, thus reducing the systematic uncertainty on the efficiency correction. In addition, the higher Pb-Pb collision centre-of-mass energy will reduce the impact of the $\sqrt{s}$-scaling of the pp reference. This will open the possibility to exploit the measurement of $\mathrm{D_s^+}$-meson production in heavy-ion collisions to assess the recombination effects in the charm-quark hadronisation and to

JHEP03(2016)082

provide further constraints to models describing the coupling of heavy quarks with the medium.

Acknowledgments

The ALICE Collaboration would like to thank all its engineers and technicians for their invaluable contributions to the construction of the experiment and the CERN accelerator teams for the outstanding performance of the LHC complex. The ALICE Collaboration gratefully acknowledges the resources and support provided by all Grid centres and the Worldwide LHC Computing Grid (WLCG) collaboration. The ALICE Collaboration would like to thank M. He, R. Fries and R. Rapp for making available their model calculations. The ALICE Collaboration acknowledges the following funding agencies for their support in building and running the ALICE detector: State Committee of Science, World Federation of Scientists (WFS) and Swiss Fonds Kidagan, Armenia; Conselho Nacional de Desenvolvimento Científico e Tecnológico (CNPq), Financiadora de Estudos e Projetos (FINEP), Fundação de Amparo à Pesquisa do Estado de São Paulo (FAPESP); National Natural Science Foundation of China (NSFC), the Chinese Ministry of Education (CMOE) and the Ministry of Science and Technology of China (MSTC); Ministry of Education and Youth of the Czech Republic; Danish Natural Science Research Council, the Carlsberg Foundation and the Danish National Research Foundation; The European Research Council under the European Community's Seventh Framework Programme; Helsinki Institute of Physics and the Academy of Finland; French CNRS-IN2P3, the 'Region Pays de Loire', 'Region Alsace', 'Region Auvergne' and CEA, France; German Bundesministerium fur Bildung, Wissenschaft, Forschung und Technologie (BMBF) and the Helmholtz Association; General Secretariat for Research and Technology, Ministry of Development, Greece; Hungarian Orszagos Tudomanyos Kutatasi Alappgrammok (OTKA) and National Office for Research and Technology (NKTH); Department of Atomic Energy and Department of Science and Technology of the Government of India; Istituto Nazionale di Fisica Nucleare (INFN) and Centro Fermi — Museo Storico della Fisica e Centro Studi e Ricerche "Enrico Fermi", Italy; MEXT Grant-in-Aid for Specially Promoted Research, Japan; Joint Institute for Nuclear Research, Dubna; National Research Foundation of Korea (NRF); Consejo Nacional de Cienca y Tecnologia (CONACYT), Direccion General de Asuntos del Personal Academico(DGAPA), México, Amerique Latine Formation academique — European Commission (ALFA-EC) and the EPLANET Program (European Particle Physics Latin American Network); Stichting voor Fundamenteel Onderzoek der Materie (FOM) and the Nederlandse Organisatie voor Wetenschappelijk Onderzoek (NWO), Netherlands; Research Council of Norway (NFR); National Science Centre, Poland; Ministry of National Education/Institute for Atomic Physics and National Council of Scientific Research in Higher Education (CNCSI-UEFISCDI), Romania; Ministry of Education and Science of Russian Federation, Russian Academy of Sciences, Russian Federal Agency of Atomic Energy, Russian Federal Agency for Science and Innovations and The Russian Foundation for Basic Research; Ministry of Education of Slovakia; Department of Science and Technology, South Africa; Centro de Investigaciones Energeticas, Medioambientales y Tecnologicas

(CIEMAT), E-Infrastructure shared between Europe and Latin America (EELA), Ministerio de Economía y Competitividad (MINECO) of Spain, Xunta de Galicia (Consellería de Educación), Centro de Aplicaciones Tecnológicas y Desarrollo Nuclear (CEADEN), Cubaenergía, Cuba, and IAEA (International Atomic Energy Agency); Swedish Research Council (VR) and Knut & Alice Wallenberg Foundation (KAW); Ukraine Ministry of Education and Science; United Kingdom Science and Technology Facilities Council (STFC); The United States Department of Energy, the United States National Science Foundation, the State of Texas, and the State of Ohio; Ministry of Science, Education and Sports of Croatia and Unity through Knowledge Fund, Croatia; Council of Scientific and Industrial Research (CSIR), New Delhi, India; Pontificia Universidad Católica del Perú.

References

[1] Wuppertal-Budapest collaboration, S. Borsányi et al., *Is there still any T_c mystery in lattice QCD? Results with physical masses in the continuum limit III*, *JHEP* **09** (2010) 073 [arXiv:1005.3508] [INSPIRE].

[2] HotQCD collaboration, A. Bazavov et al., *Equation of state in $(2+1)$-flavor QCD*, *Phys. Rev.* **D 90** (2014) 094503 [arXiv:1407.6387] [INSPIRE].

[3] T.S. Biro, E. van Doorn, B. Müller, M.H. Thoma and X.-N. Wang, *Parton equilibration in relativistic heavy ion collisions*, *Phys. Rev.* **C 48** (1993) 1275 [nucl-th/9303004] [INSPIRE].

[4] R. Vogt, *Ultrarelativistic heavy-ion collisions*, Elsevier (2007).

[5] R. Rapp and H. van Hees, *Heavy Quarks in the quark-gluon Plasma*, R.C. Hwa and X.-N. Wang eds., World Scientific (2010) [arXiv:0903.1096] [INSPIRE].

[6] N. Armesto, A. Dainese, C.A. Salgado and U.A. Wiedemann, *Testing the color charge and mass dependence of parton energy loss with heavy-to-light ratios at RHIC and CERN LHC*, *Phys. Rev.* **D 71** (2005) 054027 [hep-ph/0501225] [INSPIRE].

[7] STAR collaboration, B.I. Abelev et al., *Transverse momentum and centrality dependence of high-$p_{\rm T}$ non-photonic electron suppression in $Au+Au$ collisions at $\sqrt{s_{\rm NN}} = 200$ GeV*, *Phys. Rev. Lett.* **98** (2007) 192301 [*Erratum ibid.* **106** (2011) 159902] [nucl-ex/0607012] [INSPIRE].

[8] PHENIX collaboration, A. Adare et al., *Energy Loss and Flow of Heavy Quarks in $Au+Au$ Collisions at $\sqrt{s_{\rm NN}} = 200$ GeV*, *Phys. Rev. Lett.* **98** (2007) 172301 [nucl-ex/0611018] [INSPIRE].

[9] PHENIX collaboration, A. Adare et al., *Heavy Quark Production in $p+p$ and Energy Loss and Flow of Heavy Quarks in $Au+Au$ Collisions at $\sqrt{s_{\rm NN}} = 200$ GeV*, *Phys. Rev.* **C 84** (2011) 044905 [arXiv:1005.1627] [INSPIRE].

[10] ALICE collaboration, *Production of muons from heavy flavour decays at forward rapidity in pp and Pb-Pb collisions at $\sqrt{s_{NN}} = 2.76$ TeV*, *Phys. Rev. Lett.* **109** (2012) 112301 [arXiv:1205.6443] [INSPIRE].

JHEP03(2016)082

[11] ALICE collaboration, *Suppression of high transverse momentum D mesons in central Pb-Pb collisions at* $\sqrt{s_{\rm NN}} = 2.76$ *TeV*, *JHEP* **09** (2012) 112 [arXiv:1203.2160] [INSPIRE].

[12] STAR collaboration, L. Adamczyk et al., *Observation of* D^0 *Meson Nuclear Modifications in* $Au + Au$ *Collisions at* $\sqrt{s_{\rm NN}} = 200$ *GeV*, *Phys. Rev. Lett.* **113** (2014) 142301 [arXiv:1404.6185] [INSPIRE].

[13] CMS collaboration, *Suppression of non-prompt* J/ψ*, prompt* J/ψ *and* $\Upsilon(1S)$ *in PbPb collisions at* $\sqrt{s_{\rm NN}} = 2.76$ *TeV*, *JHEP* **05** (2012) 063 [arXiv:1201.5069] [INSPIRE].

[14] ALICE collaboration, *Measurement of prompt D-meson production in p-Pb collisions at* $\sqrt{s_{\rm NN}} = 5.02$ *TeV*, *Phys. Rev. Lett.* **113** (2014) 232301 [arXiv:1405.3452] [INSPIRE].

[15] ALICE collaboration, *D meson elliptic flow in non-central Pb-Pb collisions at* $\sqrt{s_{\rm NN}} = 2.76$ *TeV*, *Phys. Rev. Lett.* **111** (2013) 102301 [arXiv:1305.2707] [INSPIRE].

[16] ALICE collaboration, *Azimuthal anisotropy of D meson production in Pb-Pb collisions at* $\sqrt{s_{\rm NN}} = 2.76$ *TeV*, *Phys. Rev.* **C 90** (2014) 034904 [arXiv:1405.2001] [INSPIRE].

[17] STAR collaboration, L. Adamczyk et al., *Elliptic flow of non-photonic electrons in* $Au + Au$ *collisions at* $\sqrt{s_{\rm NN}} = 200$*,* 62.4 *and* 39 *GeV*, arXiv:1405.6348 [INSPIRE].

[18] D. Molnar and S.A. Voloshin, *Elliptic flow at large transverse momenta from quark coalescence*, *Phys. Rev. Lett.* **91** (2003) 092301 [nucl-th/0302014] [INSPIRE].

[19] V. Greco, C.M. Ko and P. Levai, *Parton coalescence at RHIC*, *Phys. Rev.* **C 68** (2003) 034904 [nucl-th/0305024] [INSPIRE].

[20] V. Greco, C.M. Ko and R. Rapp, *Quark coalescence for charmed mesons in ultrarelativistic heavy ion collisions*, *Phys. Lett.* **B 595** (2004) 202 [nucl-th/0312100] [INSPIRE].

[21] R.L. Thews, M. Schroedter and J. Rafelski, *Enhanced* J/ψ *production in deconfined quark matter*, *Phys. Rev.* **C 63** (2001) 054905 [hep-ph/0007323] [INSPIRE].

[22] P. Braun-Munzinger and J. Stachel, *(Non)thermal aspects of charmonium production and a new look at* J/ψ *suppression*, *Phys. Lett.* **B 490** (2000) 196 [nucl-th/0007059] [INSPIRE].

[23] ALICE collaboration, J/ψ *suppression at forward rapidity in Pb-Pb collisions at* $\sqrt{s_{\rm NN}} = 2.76$ *TeV*, *Phys. Rev. Lett.* **109** (2012) 072301 [arXiv:1202.1383] [INSPIRE].

[24] ALICE collaboration, *Centrality, rapidity and transverse momentum dependence of* J/ψ *suppression in Pb-Pb collisions at* $\sqrt{s_{\rm NN}} = 2.76$ *TeV*, *Phys. Lett.* **B 734** (2014) 314 [arXiv:1311.0214] [INSPIRE].

[25] ALICE collaboration, J/ψ *Elliptic Flow in Pb-Pb Collisions at* $\sqrt{s_{\rm NN}} = 2.76$ *TeV*, *Phys. Rev. Lett.* **111** (2013) 162301 [arXiv:1303.5880] [INSPIRE].

[26] P.B. Gossiaux, R. Bierkandt and J. Aichelin, *Tomography of a quark gluon plasma at RHIC and LHC energies*, *Phys. Rev.* **C 79** (2009) 044906 [arXiv:0901.0946] [INSPIRE].

[27] M. He, R.J. Fries and R. Rapp, *Heavy-Quark Diffusion and Hadronization in quark-gluon Plasma*, *Phys. Rev.* **C 86** (2012) 014903 [arXiv:1106.6006] [INSPIRE].

[28] S. Cao, G.-Y. Qin and S.A. Bass, *Heavy-quark dynamics and hadronization in ultrarelativistic heavy-ion collisions: Collisional versus radiative energy loss*, *Phys. Rev.* **C 88** (2013) 044907 [arXiv:1308.0617] [INSPIRE].

[29] J. Rafelski and B. Müller, *Strangeness Production in the quark-gluon Plasma*, *Phys. Rev. Lett.* **48** (1982) 1066 [*Erratum ibid.* **56** (1986) 2334] [INSPIRE].

JHEP03(2016)082

[30] P. Koch, B. Müller and J. Rafelski, *Strangeness in Relativistic Heavy Ion Collisions*, *Phys. Rept.* **142** (1986) 167 [INSPIRE].

[31] NA57 collaboration, F. Antinori et al., *Enhancement of hyperon production at central rapidity in* 158 *A GeV/c Pb-Pb collisions*, *J. Phys.* **G 32** (2006) 427 [nucl-ex/0601021] [INSPIRE].

[32] NA57 collaboration, F. Antinori et al., *Strangeness enhancements at central rapidity in* 40 *A GeV/c Pb-Pb collisions*, *J. Phys.* **G 37** (2010) 045105 [arXiv:1001.1884] [INSPIRE].

[33] NA49 collaboration, S.V. Afanasiev et al., *Energy dependence of pion and kaon production in central* $Pb + Pb$ *collisions*, *Phys. Rev.* **C 66** (2002) 054902 [nucl-ex/0205002] [INSPIRE].

[34] NA49 collaboration, C. Alt et al., *Energy dependence of* Λ *and* Ξ *production in central* $Pb + Pb$ *collisions at* 20 *A*, 30 *A*, 40 *A*, 80 *A and* 158 *A GeV measured at the CERN Super Proton Synchrotron*, *Phys. Rev.* **C 78** (2008) 034918 [arXiv:0804.3770] [INSPIRE].

[35] STAR collaboration, B.I. Abelev et al., *Enhanced strange baryon production in* $Au + Au$ *collisions compared to* $p + p$ *at* $\sqrt{s_{\rm NN}} = 200$ *GeV*, *Phys. Rev.* **C 77** (2008) 044908 [arXiv:0705.2511] [INSPIRE].

[36] ALICE collaboration, *Multi-strange baryon production at mid-rapidity in Pb-Pb collisions at* $\sqrt{s_{\rm NN}} = 2.76$ *TeV*, *Phys. Lett.* **B 728** (2014) 216 [*Erratum ibid.* **B 734** (2014) 409] [arXiv:1307.5543] [INSPIRE].

[37] S. Hamieh, K. Redlich and A. Tounsi, *Canonical description of strangeness enhancement from p-A to Pb-Pb collisions*, *Phys. Lett.* **B 486** (2000) 61 [hep-ph/0006024] [INSPIRE].

[38] P. Braun-Munzinger, K. Redlich and J. Stachel, *Particle production in heavy ion collisions*, nucl-th/0304013 [INSPIRE].

[39] A. Andronic, P. Braun-Munzinger, K. Redlich and J. Stachel, *Statistical hadronization of charm in heavy ion collisions at SPS, RHIC and LHC*, *Phys. Lett.* **B 571** (2003) 36 [nucl-th/0303036] [INSPIRE].

[40] I. Kuznetsova and J. Rafelski, *Heavy flavor hadrons in statistical hadronization of strangeness-rich QGP*, *Eur. Phys. J.* **C 51** (2007) 113 [hep-ph/0607203] [INSPIRE].

[41] M. He, R.J. Fries and R. Rapp, D_s*-Meson as Quantitative Probe of Diffusion and Hadronization in Nuclear Collisions*, *Phys. Rev. Lett.* **110** (2013) 112301 [arXiv:1204.4442] [INSPIRE].

[42] ALICE collaboration, *Transverse momentum dependence of D-meson production in Pb-Pb collisions at* $\sqrt{s_{\rm NN}} = 2.76$ *TeV*, arXiv:1509.06888 [INSPIRE].

[43] S. Wicks, W. Horowitz, M. Djordjevic and M. Gyulassy, *Heavy quark jet quenching with collisional plus radiative energy loss and path length fluctuations*, *Nucl. Phys.* **A 783** (2007) 493 [nucl-th/0701063] [INSPIRE].

[44] M. Djordjevic, *Heavy flavor puzzle at LHC: a serendipitous interplay of jet suppression and fragmentation*, *Phys. Rev. Lett.* **112** (2014) 042302 [arXiv:1307.4702] [INSPIRE].

[45] ALICE collaboration, D_s^+ *meson production at central rapidity in proton-proton collisions at* $\sqrt{s} = 7$ *TeV*, *Phys. Lett.* **B 718** (2012) 279 [arXiv:1208.1948] [INSPIRE].

[46] ALICE collaboration, *The ALICE experiment at the CERN LHC*, 2008 *JINST* **3** S08002 [INSPIRE].

JHEP03(2016)082

[47] ALICE collaboration, *Performance of the ALICE Experiment at the CERN LHC*, *Int. J. Mod. Phys.* **A 29** (2014) 1430044 [arXiv:1402.4476] [INSPIRE].

[48] R.J. Glauber, *Cross-sections in deuterium at high-energies*, *Phys. Rev.* **100** (1955) 242 [INSPIRE].

[49] R.J. Glauber and G. Matthiae, *High-energy scattering of protons by nuclei*, *Nucl. Phys.* **B 21** (1970) 135 [INSPIRE].

[50] M.L. Miller, K. Reygers, S.J. Sanders and P. Steinberg, *Glauber modeling in high energy nuclear collisions*, *Ann. Rev. Nucl. Part. Sci.* **57** (2007) 205 [nucl-ex/0701025] [INSPIRE].

[51] ALICE collaboration, *Centrality determination of Pb-Pb collisions at* $\sqrt{s_{\rm NN}} = 2.76$ *TeV with ALICE*, *Phys. Rev.* **C 88** (2013) 044909 [arXiv:1301.4361] [INSPIRE].

[52] Particle Data Group collaboration, K.A. Olive et al., *Review of Particle Physics*, *Chin. Phys.* **C 38** (2014) 090001 [INSPIRE].

[53] ALICE collaboration, *Measurement of charm production at central rapidity in proton-proton collisions at* $\sqrt{s} = 7$ *TeV*, *JHEP* **01** (2012) 128 [arXiv:1111.1553] [INSPIRE].

[54] X.-N. Wang and M. Gyulassy, *HIJING: A Monte Carlo model for multiple jet production in pp, pA and AA collisions*, *Phys. Rev.* **D 44** (1991) 3501 [INSPIRE].

[55] T. Sjöstrand, S. Mrenna and P.Z. Skands, *PYTHIA 6.4 Physics and Manual*, *JHEP* **05** (2006) 026 [hep-ph/0603175] [INSPIRE].

[56] M. Cacciari, M. Greco and P. Nason, *The* $p_{\rm T}$ *spectrum in heavy flavor hadroproduction*, *JHEP* **05** (1998) 007 [hep-ph/9803400] [INSPIRE].

[57] M. Cacciari, S. Frixione, N. Houdeau, M.L. Mangano, P. Nason and G. Ridolfi, *Theoretical predictions for charm and bottom production at the LHC*, *JHEP* **10** (2012) 137 [arXiv:1205.6344] [INSPIRE].

[58] J. Uphoff, O. Fochler, Z. Xu and C. Greiner, *Open Heavy Flavor in* $Pb + Pb$ *Collisions at* $\sqrt{s} = 2.76$ *TeV within a Transport Model*, *Phys. Lett.* **B 717** (2012) 430 [arXiv:1205.4945] [INSPIRE].

[59] R. Brun, F. Carminati and S. Giani, *GEANT Detector Description and Simulation Tool*, CERN-W5013, (1994) [INSPIRE].

[60] D.J. Lange, *The EvtGen particle decay simulation package*, *Nucl. Instrum. Meth.* **A 462** (2001) 152 [INSPIRE].

[61] M. He, R.J. Fries and R. Rapp, *Heavy Flavor at the Large Hadron Collider in a Strong Coupling Approach*, *Phys. Lett.* **B 735** (2014) 445 [arXiv:1401.3817] [INSPIRE].

[62] R. Averbeck, N. Bastid, Z.C. del Valle, P. Crochet, A. Dainese and X. Zhang, *Reference Heavy Flavour Cross Sections in pp Collisions at* $\sqrt{s} = 2.76$ *TeV, using a pQCD-Driven* $\sqrt{s}$*-Scaling of ALICE Measurements at* $\sqrt{s} = 7$ *TeV*, arXiv:1107.3243 [INSPIRE].

[63] ALICE collaboration, *Measurement of charm production at central rapidity in proton-proton collisions at* $\sqrt{s} = 2.76$ *TeV*, *JHEP* **07** (2012) 191 [arXiv:1205.4007] [INSPIRE].

[64] E. Braaten, K.-m. Cheung, S. Fleming and T.C. Yuan, *Perturbative QCD fragmentation functions as a model for heavy quark fragmentation*, *Phys. Rev.* **D 51** (1995) 4819 [hep-ph/9409316] [INSPIRE].

[65] ALICE collaboration, *Inclusive, prompt and non-prompt* J/ψ *production at mid-rapidity in Pb-Pb collisions at* $\sqrt{s_{\rm NN}} = 2.76$ *TeV*, *JHEP* **07** (2015) 051 [arXiv:1504.07151] [INSPIRE].

JHEP03(2016)082

[66] ALICE collaboration, *Centrality dependence of high-p_T D meson suppression in Pb-Pb collisions at $\sqrt{s_{\rm NN}} = 2.76$ TeV*, *JHEP* **11** (2015) 205 [arXiv:1506.06604] [INSPIRE].

[67] A. Andronic, P. Braun-Munzinger, K. Redlich and J. Stachel, *Statistical hadronization model predictions for charmed hadrons at LHC*, in *Workshop on Heavy Ion Collisions at the LHC: Last Call for Predictions*, Geneva, Switzerland, May 14–June 8 2007 [arXiv:0707.4075] [INSPIRE].

[68] N. Armesto et al., *Heavy Ion Collisions at the LHC — Last Call for Predictions*, *J. Phys.* **G 35** (2008) 054001 [arXiv:0711.0974] [INSPIRE].

[69] J. Stachel, A. Andronic, P. Braun-Munzinger and K. Redlich, *Confronting LHC data with the statistical hadronization model*, *J. Phys. Conf. Ser.* **509** (2014) 012019 [arXiv:1311.4662] [INSPIRE].

JHEP03(2016)082

The ALICE collaboration

J. Adam[40] , D. Adamová[83] , M.M. Aggarwal[87] , G. Aglieri Rinella[36] , M. Agnello[110] , N. Agrawal[48] , Z. Ahammed[132] , S.U. Ahn[68] , S. Aiola[136] , A. Akindinov[58] , S.N. Alam[132] , D. Aleksandrov[99] , B. Alessandro[110] , D. Alexandre[101] , R. Alfaro Molina[64] , A. Alici[12,104] , A. Alkin[3] , J.R.M. Almaraz[119] , J. Alme[38] , T. Alt[43] , S. Altinpinar[18] , I. Altsybeev[131] , C. Alves Garcia Prado[120] , C. Andrei[78] , A. Andronic[96] , V. Anguelov[93] , J. Anielski[54] , T. Antičić[97] , F. Antinori[107] , P. Antonioli[104] , L. Aphecetche[113] , H. Appelshäuser[53] , S. Arcelli[28] , R. Arnaldi[110] , O.W. Arnold[37,92] , I.C. Arsene[22] , M. Arslandok[53] , B. Audurier[113] , A. Augustinus[36] , R. Averbeck[96] , M.D. Azmi[19] , A. Badalà[106] , Y.W. Baek[67,44] , S. Bagnasco[110] , R. Bailhache[53] , R. Bala[90] , A. Baldisseri[15] , R.C. Baral[61] , A.M. Barbano[27] , R. Barbera[29] , F. Barile[33] , G.G. Barnaföldi[135] , L.S. Barnby[101] , V. Barret[70] , P. Bartalini[7] , K. Barth[36] , J. Bartke[117] , E. Bartsch[53] , M. Basile[28] , N. Bastid[70] , S. Basu[132] , B. Bathen[54] , G. Batigne[113] , A. Batista Camejo[70] , B. Batyunya[66] , P.C. Batzing[22] , I.G. Bearden[80] , H. Beck[53] , C. Bedda[110] , N.K. Behera[50] , I. Belikov[55] , F. Bellini[28] , H. Bello Martinez[2] , R. Bellwied[122] , R. Belmont[134] , E. Belmont-Moreno[64] , V. Belyaev[75] , G. Bencedi[135] , S. Beole[27] , I. Berceanu[78] , A. Bercuci[78] , Y. Berdnikov[85] , D. Berenyi[135] , R.A. Bertens[57] , D. Berzano[36] , L. Betev[36] , A. Bhasin[90] , I.R. Bhat[90] , A.K. Bhati[87] , B. Bhattacharjee[45] , J. Bhom[128] , L. Bianchi[122] , N. Bianchi[72] , C. Bianchin[57,134] , J. Bielčík[40] , J. Bielčíková[83] , A. Bilandzic[80] , R. Biswas[4] , S. Biswas[79] , S. Bjelogrlic[57] , J.T. Blair[118] , D. Blau[99] , C. Blume[53] , F. Bock[93,74] , A. Bogdanov[75] , H. Bøggild[80] , L. Boldizsár[135] , M. Bombara[41] , J. Book[53] , H. Borel[15] , A. Borissov[95] , M. Borri[82,124] , F. Bossú[65] , E. Botta[27] , S. Böttger[52] , C. Bourjau[80] , P. Braun-Munzinger[96] , M. Bregant[120] , T. Breitner[52] , T.A. Broker[53] , T.A. Browning[94] , M. Broz[40] , E.J. Brucken[46] , E. Bruna[110] , G.E. Bruno[33] , D. Budnikov[98] , H. Buesching[53] , S. Bufalino[27,36] , P. Buncic[36] , O. Busch[93,128] , Z. Buthelezi[65] , J.B. Butt[16] , J.T. Buxton[20] , D. Caffarri[36] , X. Cai[7] , H. Caines[136] , L. Calero Diaz[72] , A. Caliva[57] , E. Calvo Villar[102] , P. Camerini[26] , F. Carena[36] , W. Carena[36] , F. Carnesecchi[28] , J. Castillo Castellanos[15] , A.J. Castro[125] , E.A.R. Casula[25] , C. Ceballos Sanchez[9] , J. Cepila[40] , P. Cerello[110] , J. Cerkala[115] , B. Chang[123] , S. Chapeland[36] , M. Chartier[124] , J.L. Charvet[15] , S. Chattopadhyay[132] , S. Chattopadhyay[100] , V. Chelnokov[3] , M. Cherney[86] , C. Cheshkov[130] , B. Cheynis[130] , V. Chibante Barroso[36] , D.D. Chinellato[121] , S. Cho[50] , P. Chochula[36] , K. Choi[95] , M. Chojnacki[80] , S. Choudhury[132] , P. Christakoglou[81] , C.H. Christensen[80] , P. Christiansen[34] , T. Chujo[128] , S.U. Chung[95] , C. Cicalo[105] , L. Cifarelli[12,28] , F. Cindolo[104] , J. Cleymans[89] , F. Colamaria[33] , D. Colella[33,36] , A. Collu[74,25] , M. Colocci[28] , G. Conesa Balbastre[71] , Z. Conesa del Valle[51] , M.E. Connors[ii,136] , J.G. Contreras[40] , T.M. Cormier[84] , Y. Corrales Morales[110] , I. Cortés Maldonado[2] , P. Cortese[32] , M.R. Cosentino[120] , F. Costa[36] , P. Crochet[70] , R. Cruz Albino[11] , E. Cuautle[63] , L. Cunqueiro[36] , T. Dahms[92,37] , A. Dainese[107] , A. Danu[62] , D. Das[100] , I. Das[51,100] , S. Das[4] , A. Dash[121,79] , S. Dash[48] , S. De[120] , A. De Caro[31,12] , G. de Cataldo[103] , C. de Conti[120] , J. de Cuveland[43] , A. De Falco[25] , D. De Gruttola[12,31] , N. De Marco[110] , S. De Pasquale[31] , A. Deisting[96,93] , A. Deloff[77] , E. Dénes[135,i], C. Deplano[81] , P. Dhankher[48] , D. Di Bari[33] , A. Di Mauro[36] , P. Di Nezza[72] , M.A. Diaz Corchero[10] , T. Dietel[89] , P. Dillenseger[53] , R. Divià[36] , Ø. Djuvsland[18] , A. Dobrin[57,81] , D. Domenicis Gimenez[120] , B. Dönigus[53] , O. Dordic[22] , T. Drozhzhova[53] , A.K. Dubey[132] , A. Dubla[57] , L. Ducroux[130] , P. Dupieux[70] , R.J. Ehlers[136] , D. Elia[103] , H. Engel[52] , E. Epple[136] , B. Erazmus[113] , I. Erdemir[53] , F. Erhardt[129] , B. Espagnon[51] , M. Estienne[113] , S. Esumi[128] , J. Eum[95] , D. Evans[101] , S. Evdokimov[111] , G. Eyyubova[40] , L. Fabbietti[92,37] , D. Fabris[107] , J. Faivre[71] , A. Fantoni[72] , M. Fasel[74] , L. Feldkamp[54] , A. Feliciello[110] , G. Feofilov[131] , J. Ferencei[83] , A. Fernández Téllez[2] , E.G. Ferreiro[17] , A. Ferretti[27] , A. Festanti[30] , V.J.G. Feuillard[15,70] , J. Figiel[117] , M.A.S. Figueredo[124,120] , S. Filchagin[98] , D. Finogeev[56] , F.M. Fionda[25] , E.M. Fiore[33] , M.G. Fleck[93] , M. Floris[36] ,

JHEP03(2016)082

S. Foertsch[65], P. Foka[96], S. Fokin[99], E. Fragiacomo[109], A. Francescon[30,36], U. Frankenfeld[96], U. Fuchs[36], C. Furget[71], A. Furs[56], M. Fusco Girard[31], J.J. Gaardhøje[80], M. Gagliardi[27], A.M. Gago[102], M. Gallio[27], D.R. Gangadharan[74], P. Ganoti[36,88], C. Gao[7], C. Garabatos[96], E. Garcia-Solis[13], C. Gargiulo[36], P. Gasik[37,92], E.F. Gauger[118], M. Germain[113], A. Gheata[36], M. Gheata[62,36], P. Ghosh[132], S.K. Ghosh[4], P. Gianotti[72], P. Giubellino[36,110], P. Giubilato[30], E. Gladysz-Dziadus[117], P. Glässel[93], D.M. Goméz Coral[64], A. Gomez Ramirez[52], V. Gonzalez[10], P. González-Zamora[10], S. Gorbunov[43], L. Görlich[117], S. Gotovac[116], V. Grabski[64], O.A. Grachov[136], L.K. Graczykowski[133], K.L. Graham[101], A. Grelli[57], A. Grigoras[36], C. Grigoras[36], V. Grigoriev[75], A. Grigoryan[1], S. Grigoryan[66], B. Grinyov[3], N. Grion[109], J.M. Gronefeld[96], J.F. Grosse-Oetringhaus[36], J.-Y. Grossiord[130], R. Grosso[96], F. Guber[56], R. Guernane[71], B. Guerzoni[28], K. Gulbrandsen[80], T. Gunji[127], A. Gupta[90], R. Gupta[90], R. Haake[54], Ø. Haaland[18], C. Hadjidakis[51], M. Haiduc[62], H. Hamagaki[127], G. Hamar[135], J.W. Harris[136], A. Harton[13], D. Hatzifotiadou[104], S. Hayashi[127], S.T. Heckel[53], M. Heide[54], H. Helstrup[38], A. Herghelegiu[78], G. Herrera Corral[11], B.A. Hess[35], K.F. Hetland[38], H. Hillemanns[36], B. Hippolyte[55], R. Hosokawa[128], P. Hristov[36], M. Huang[18], T.J. Humanic[20], N. Hussain[45], T. Hussain[19], D. Hutter[43], D.S. Hwang[21], R. Ilkaev[98], M. Inaba[128], G.M. Innocenti[27], M. Ippolitov[75,99], M. Irfan[19], M. Ivanov[96], V. Ivanov[85], V. Izucheev[111], P.M. Jacobs[74], M.B. Jadhav[48], S. Jadlovska[115], J. Jadlovsky[115,59], C. Jahnke[120], M.J. Jakubowska[133], H.J. Jang[68], M.A. Janik[133], P.H.S.Y. Jayarathna[122], C. Jena[30], S. Jena[122], R.T. Jimenez Bustamante[96], P.G. Jones[101], H. Jung[44], A. Jusko[101], P. Kalinak[59], A. Kalweit[36], J. Kamin[53], J.H. Kang[137], V. Kaplin[75], S. Kar[132], A. Karasu Uysal[69], O. Karavichev[56], T. Karavicheva[56], L. Karayan[96,93], E. Karpechev[56], U. Kebschull[52], R. Keidel[138], D.L.D. Keijdener[57], M. Keil[36], M. Mohisin Khan[19], P. Khan[100], S.A. Khan[132], A. Khanzadeev[85], Y. Kharlov[111], B. Kileng[38], D.W. Kim[44], D.J. Kim[123], D. Kim[137], H. Kim[137], J.S. Kim[44], M. Kim[44], M. Kim[137], S. Kim[21], T. Kim[137], S. Kirsch[43], I. Kisel[43], S. Kiselev[58], A. Kisiel[133], G. Kiss[135], J.L. Klay[6], C. Klein[53], J. Klein[36,93], C. Klein-Bösing[54], S. Klewin[93], A. Kluge[36], M.L. Knichel[93], A.G. Knospe[118], T. Kobayashi[128], C. Kobdaj[114], M. Kofarago[36], T. Kollegger[96,43], A. Kolojvari[131], V. Kondratiev[131], N. Kondratyeva[75], E. Kondratyuk[111], A. Konevskikh[56], M. Kopcik[115], M. Kour[90], C. Kouzinopoulos[36], O. Kovalenko[77], V. Kovalenko[131], M. Kowalski[117], G. Koyithatta Meethaleveedu[48], I. Králik[59], A. Kravčáková[41], M. Kretz[43], M. Krivda[59,101], F. Krizek[83], E. Kryshen[36], M. Krzewicki[43], A.M. Kubera[20], V. Kučera[83], C. Kuhn[55], P.G. Kuijer[81], A. Kumar[90], J. Kumar[48], L. Kumar[87], S. Kumar[48], P. Kurashvili[77], A. Kurepin[56], A.B. Kurepin[56], A. Kuryakin[98], M.J. Kweon[50], Y. Kwon[137], S.L. La Pointe[110], P. La Rocca[29], P. Ladron de Guevara[11], C. Lagana Fernandes[120], I. Lakomov[36], R. Langoy[42], C. Lara[52], A. Lardeux[15], A. Lattuca[27], E. Laudi[36], R. Lea[26], L. Leardini[93], G.R. Lee[101], S. Lee[137], F. Lehas[81], R.C. Lemmon[82], V. Lenti[103], E. Leogrande[57], I. León Monzón[119], H. León Vargas[64], M. Leoncino[27], P. Lévai[135], S. Li[70,7], X. Li[14], J. Lien[42], R. Lietava[101], S. Lindal[22], V. Lindenstruth[43], C. Lippmann[96], M.A. Lisa[20], H.M. Ljunggren[34], D.F. Lodato[57], P.I. Loenne[18], V. Loginov[75], C. Loizides[74], X. Lopez[70], E. López Torres[9], A. Lowe[135], P. Luettig[53], M. Lunardon[30], G. Luparello[26], A. Maevskaya[56], M. Mager[36], S. Mahajan[90], S.M. Mahmood[22], A. Maire[55], R.D. Majka[136], M. Malaev[85], I. Maldonado Cervantes[63], L. Malinina[iii,66], D. Mal'Kevich[58], P. Malzacher[96], A. Mamonov[98], V. Manko[99], F. Manso[70], V. Manzari[36,103], M. Marchisone[27,65,126], J. Mareš[60], G.V. Margagliotti[26], A. Margotti[104], J. Margutti[57], A. Marín[96], C. Markert[118], M. Marquard[53], N.A. Martin[96], J. Martin Blanco[113], P. Martinengo[36], M.I. Martínez[2], G. Martínez García[113], M. Martinez Pedreira[36], A. Mas[120], S. Masciocchi[96], M. Masera[27], A. Masoni[105], L. Massacrier[113], A. Mastroserio[33], A. Matyja[117], C. Mayer[117], J. Mazer[125], M.A. Mazzoni[108], D. Mcdonald[122], F. Meddi[24], Y. Melikyan[75], A. Menchaca-Rocha[64], E. Meninno[31], J. Mercado Pérez[93], M. Meres[39],

JHEP03(2016)082

Y. Miake[128] , M.M. Mieskolainen[46] , K. Mikhaylov[66,58] , L. Milano[36] , J. Milosevic[22] , L.M. Minervini[103,23] , A. Mischke[57] , A.N. Mishra[49] , D. Miśkowiec[96] , J. Mitra[132] , C.M. Mitu[62] , N. Mohammadi[57] , B. Mohanty[79,132] , L. Molnar[55,113] , L. Montaño Zetina[11] , E. Montes[10] , D.A. Moreira De Godoy[54,113] , L.A.P. Moreno[2] , S. Moretto[30] , A. Morreale[113] , A. Morsch[36] , V. Muccifora[72] , E. Mudnic[116] , D. Mühlheim[54] , S. Muhuri[132] , M. Mukherjee[132] , J.D. Mulligan[136] , M.G. Munhoz[120] , R.H. Munzer[92,37] , S. Murray[65] , L. Musa[36] , J. Musinsky[59] , B. Naik[48] , R. Nair[77] , B.K. Nandi[48] , R. Nania[104] , E. Nappi[103] , M.U. Naru[16] , H. Natal da Luz[120] , C. Nattrass[125] , K. Nayak[79] , T.K. Nayak[132] , S. Nazarenko[98] , A. Nedosekin[58] , L. Nellen[63] , F. Ng[122] , M. Nicassio[96] , M. Niculescu[62] , J. Niedziela[36] , B.S. Nielsen[80] , S. Nikolaev[99] , S. Nikulin[99] , V. Nikulin[85] , F. Noferini[12,104] , P. Nomokonov[66] , G. Nooren[57] , J.C.C. Noris[2] , J. Norman[124] , A. Nyanin[99] , J. Nystrand[18] , H. Oeschler[93] , S. Oh[136] , S.K. Oh[67] , A. Ohlson[36] , A. Okatan[69] , T. Okubo[47] , L. Olah[135] , J. Oleniacz[133] , A.C. Oliveira Da Silva[120] , M.H. Oliver[136] , J. Onderwaater[96] , C. Oppedisano[110] , R. Orava[46] , A. Ortiz Velasquez[63] , A. Oskarsson[34] , J. Otwinowski[117] , K. Oyama[93,76] , M. Ozdemir[53] , Y. Pachmayer[93] , P. Pagano[31] , G. Paić[63] , S.K. Pal[132] , J. Pan[134] , A.K. Pandey[48] , P. Papcun[115] , V. Papikyan[1] , G.S. Pappalardo[106] , P. Pareek[49] , W.J. Park[96] , S. Parmar[87] , A. Passfeld[54] , V. Paticchio[103] , R.N. Patra[132] , B. Paul[100] , T. Peitzmann[57] , H. Pereira Da Costa[15] , E. Pereira De Oliveira Filho[120] , D. Peresunko[99,75] , C.E. Pérez Lara[81] , E. Perez Lezama[53] , V. Peskov[53] , Y. Pestov[5] , V. Petráček[40] , V. Petrov[111] , M. Petrovici[78] , C. Petta[29] , S. Piano[109] , M. Pikna[39] , P. Pillot[113] , O. Pinazza[104,36] , L. Pinsky[122] , D.B. Piyarathna[122] , M. Płoskoń[74] , M. Planinic[129] , J. Pluta[133] , S. Pochybova[135] , P.L.M. Podesta-Lerma[119] , M.G. Poghosyan[84,86] , B. Polichtchouk[111] , N. Poljak[129] , W. Poonsawat[114] , A. Pop[78] , S. Porteboeuf-Houssais[70] , J. Porter[74] , J. Pospisil[83] , S.K. Prasad[4] , R. Preghenella[36,104] , F. Prino[110] , C.A. Pruneau[134] , I. Pshenichnov[56] , M. Puccio[27] , G. Puddu[25] , P. Pujahari[134] , V. Punin[98] , J. Putschke[134] , H. Qvigstad[22] , A. Rachevski[109] , S. Raha[4] , S. Rajput[90] , J. Rak[123] , A. Rakotozafindrabe[15] , L. Ramello[32] , F. Rami[55] , R. Raniwala[91] , S. Raniwala[91] , S.S. Räsänen[46] , B.T. Rascanu[53] , D. Rathee[87] , K.F. Read[125,84] , K. Redlich[77] , R.J. Reed[134] , A. Rehman[18] , P. Reichelt[53] , F. Reidt[93,36] , X. Ren[7] , R. Renfordt[53] , A.R. Reolon[72] , A. Reshetin[56] , J.-P. Revol[12] , K. Reygers[93] , V. Riabov[85] , R.A. Ricci[73] , T. Richert[34] , M. Richter[22] , P. Riedler[36] , W. Riegler[36] , F. Riggi[29] , C. Ristea[62] , E. Rocco[57] , M. Rodríguez Cahuantzi[2,11] , A. Rodriguez Manso[81] , K. Røed[22] , E. Rogochaya[66] , D. Rohr[43] , D. Röhrich[18] , R. Romita[124] , F. Ronchetti[72,36] , L. Ronflette[113] , P. Rosnet[70] , A. Rossi[30,36] , F. Roukoutakis[88] , A. Roy[49] , C. Roy[55] , P. Roy[100] , A.J. Rubio Montero[10] , R. Rui[26] , R. Russo[27] , E. Ryabinkin[99] , Y. Ryabov[85] , A. Rybicki[117] , S. Sadovsky[111] , K. Šafařík[36] , B. Sahlmuller[53] , P. Sahoo[49] , R. Sahoo[49] , S. Sahoo[61] , P.K. Sahu[61] , J. Saini[132] , S. Sakai[72] , M.A. Saleh[134] , J. Salzwedel[20] , S. Sambyal[90] , V. Samsonov[85] , L. Šándor[59] , A. Sandoval[64] , M. Sano[128] , D. Sarkar[132] , E. Scapparone[104] , F. Scarlassara[30] , C. Schiaua[78] , R. Schicker[93] , C. Schmidt[96] , H.R. Schmidt[35] , S. Schuchmann[53] , J. Schukraft[36] , M. Schulc[40] , T. Schuster[136] , Y. Schutz[36,113] , K. Schwarz[96] , K. Schweda[96] , G. Scioli[28] , E. Scomparin[110] , R. Scott[125] , M. Šefčík[41] , J.E. Seger[86] , Y. Sekiguchi[127] , D. Sekihata[47] , I. Selyuzhenkov[96] , K. Senosi[65] , S. Senyukov[3,36] , E. Serradilla[10,64] , A. Sevcenco[62] , A. Shabanov[56] , A. Shabetai[113] , O. Shadura[3] , R. Shahoyan[36] , A. Shangaraev[111] , A. Sharma[90] , M. Sharma[90] , M. Sharma[90] , N. Sharma[125] , K. Shigaki[47] , K. Shtejer[9,27] , Y. Sibiriak[99] , S. Siddhanta[105] , K.M. Sielewicz[36] , T. Siemiarczuk[77] , D. Silvermyr[84,34] , C. Silvestre[71] , G. Simatovic[129] , G. Simonetti[36] , R. Singaraju[132] , R. Singh[79] , S. Singha[132,79] , V. Singhal[132] , B.C. Sinha[132] , T. Sinha[100] , B. Sitar[39] , M. Sitta[32] , T.B. Skaali[22] , M. Slupecki[123] , N. Smirnov[136] , R.J.M. Snellings[57] , T.W. Snellman[123] , C. Søgaard[34] , J. Song[95] , M. Song[137] , Z. Song[7] , F. Soramel[30] , S. Sorensen[125] , F. Sozzi[96] , M. Spacek[40] , E. Spiriti[72] , I. Sputowska[117] , M. Spyropoulou-Stassinaki[88] , J. Stachel[93] , I. Stan[62] , G. Stefanek[77] , E. Stenlund[34] , G. Steyn[65] ,

JHEP03(2016)082

J.H. Stiller[93] , D. Stocco[113] , P. Strmen[39] , A.A.P. Suaide[120] , T. Sugitate[47] , C. Suire[51] , M. Suleymanov[16] , M. Suljic[26,i], R. Sultanov[58] , M. Šumbera[83] , A. Szabo[39] , A. Szanto de Toledo[120,i], I. Szarka[39] , A. Szczepankiewicz[36] , M. Szymanski[133] , U. Tabassam[16] , J. Takahashi[121] , G.J. Tambave[18] , N. Tanaka[128] , M.A. Tangaro[33] , M. Tarhini[51] , M. Tariq[19] , M.G. Tarzila[78] , A. Tauro[36] , G. Tejeda Muñoz[2] , A. Telesca[36] , K. Terasaki[127] , C. Terrevoli[30] , B. Teyssier[130] , J. Thäder[74] , D. Thomas[118] , R. Tieulent[130] , A.R. Timmins[122] , A. Toia[53] , S. Trogolo[27] , G. Trombetta[33] , V. Trubnikov[3] , W.H. Trzaska[123] , T. Tsuji[127] , A. Tumkin[98] , R. Turrisi[107] , T.S. Tveter[22] , K. Ullaland[18] , A. Uras[130] , G.L. Usai[25] , A. Utrobicic[129] , M. Vajzer[83] , M. Vala[59] , L. Valencia Palomo[70] , S. Vallero[27] , J. Van Der Maarel[57] , J.W. Van Hoorne[36] , M. van Leeuwen[57] , T. Vanat[83] , P. Vande Vyvre[36] , D. Varga[135] , A. Vargas[2] , M. Vargyas[123] , R. Varma[48] , M. Vasileiou[88] , A. Vasiliev[99] , A. Vauthier[71] , V. Vechernin[131] , A.M. Veen[57] , M. Veldhoen[57] , A. Velure[18] , M. Venaruzzo[73] , E. Vercellin[27] , S. Vergara Limón[2] , R. Vernet[8] , M. Verweij[134] , L. Vickovic[116] , G. Viesti[30,i], J. Viinikainen[123] , Z. Vilakazi[126] , O. Villalobos Baillie[101] , A. Villatoro Tello[2] , A. Vinogradov[99] , L. Vinogradov[131] , Y. Vinogradov[98,i], T. Virgili[31] , V. Vislavicius[34] , Y.P. Viyogi[132] , A. Vodopyanov[66] , M.A. Völkl[93] , K. Voloshin[58] , S.A. Voloshin[134] , G. Volpe[135] , B. von Haller[36] , I. Vorobyev[37,92] , D. Vranic[96,36] , J. Vrláková[41] , B. Vulpescu[70] , A. Vyushin[98] , B. Wagner[18] , J. Wagner[96] , H. Wang[57] , M. Wang[7,113] , D. Watanabe[128] , Y. Watanabe[127] , M. Weber[112,36] , S.G. Weber[96] , D.F. Weiser[93] , J.P. Wessels[54] , U. Westerhoff[54] , A.M. Whitehead[89] , J. Wiechula[35] , J. Wikne[22] , M. Wilde[54] , G. Wilk[77] , J. Wilkinson[93] , M.C.S. Williams[104] , B. Windelband[93] , M. Winn[93] , C.G. Yaldo[134] , H. Yang[57] , P. Yang[7] , S. Yano[47] , C. Yasar[69] , Z. Yin[7] , H. Yokoyama[128] , I.-K. Yoo[95] , J.H. Yoon[50] , V. Yurchenko[3] , I. Yushmanov[99] , A. Zaborowska[133] , V. Zaccolo[80] , A. Zaman[16] , C. Zampolli[104] , H.J.C. Zanoli[120] , S. Zaporozhets[66] , N. Zardoshti[101] , A. Zarochentsev[131] , P. Závada[60] , N. Zaviyalov[98] , H. Zbroszczyk[133] , I.S. Zgura[62] , M. Zhalov[85] , H. Zhang[18] , X. Zhang[74] , Y. Zhang[7] , C. Zhang[57] , Z. Zhang[7] , C. Zhao[22] , N. Zhigareva[58] , D. Zhou[7] , Y. Zhou[80] , Z. Zhou[18] , H. Zhu[18] , J. Zhu[113,7] , A. Zichichi[28,12] , A. Zimmermann[93] , M.B. Zimmermann[54,36] , G. Zinovjev[3] , M. Zyzak[43]

[i] *Deceased*
[ii] *Also at: Georgia State University, Atlanta, Georgia, United States*
[iii] *Also at: M.V. Lomonosov Moscow State University, D.V. Skobeltsyn Institute of Nuclear, Physics, Moscow, Russia*

[1] *A.I. Alikhanyan National Science Laboratory (Yerevan Physics Institute) Foundation, Yerevan, Armenia*
[2] *Benemérita Universidad Autónoma de Puebla, Puebla, Mexico*
[3] *Bogolyubov Institute for Theoretical Physics, Kiev, Ukraine*
[4] *Bose Institute, Department of Physics and Centre for Astroparticle Physics and Space Science (CAPSS), Kolkata, India*
[5] *Budker Institute for Nuclear Physics, Novosibirsk, Russia*
[6] *California Polytechnic State University, San Luis Obispo, California, United States*
[7] *Central China Normal University, Wuhan, China*
[8] *Centre de Calcul de l'IN2P3, Villeurbanne, France*
[9] *Centro de Aplicaciones Tecnológicas y Desarrollo Nuclear (CEADEN), Havana, Cuba*
[10] *Centro de Investigaciones Energéticas Medioambientales y Tecnológicas (CIEMAT), Madrid, Spain*
[11] *Centro de Investigación y de Estudios Avanzados (CINVESTAV), Mexico City and Mérida, Mexico*
[12] *Centro Fermi - Museo Storico della Fisica e Centro Studi e Ricerche "Enrico Fermi", Rome, Italy*
[13] *Chicago State University, Chicago, Illinois, U.S.A.*
[14] *China Institute of Atomic Energy, Beijing, China*

JHEP03(2016)082

[15] *Commissariat à l'Energie Atomique, IRFU, Saclay, France*
[16] *COMSATS Institute of Information Technology (CIIT), Islamabad, Pakistan*
[17] *Departamento de Física de Partículas and IGFAE, Universidad de Santiago de Compostela, Santiago de Compostela, Spain*
[18] *Department of Physics and Technology, University of Bergen, Bergen, Norway*
[19] *Department of Physics, Aligarh Muslim University, Aligarh, India*
[20] *Department of Physics, Ohio State University, Columbus, Ohio, United States*
[21] *Department of Physics, Sejong University, Seoul, South Korea*
[22] *Department of Physics, University of Oslo, Oslo, Norway*
[23] *Dipartimento di Elettrotecnica ed Elettronica del Politecnico, Bari, Italy*
[24] *Dipartimento di Fisica dell'Università 'La Sapienza' and Sezione INFN Rome, Italy*
[25] *Dipartimento di Fisica dell'Università and Sezione INFN, Cagliari, Italy*
[26] *Dipartimento di Fisica dell'Università and Sezione INFN, Trieste, Italy*
[27] *Dipartimento di Fisica dell'Università and Sezione INFN, Turin, Italy*
[28] *Dipartimento di Fisica e Astronomia dell'Università and Sezione INFN, Bologna, Italy*
[29] *Dipartimento di Fisica e Astronomia dell'Università and Sezione INFN, Catania, Italy*
[30] *Dipartimento di Fisica e Astronomia dell'Università and Sezione INFN, Padova, Italy*
[31] *Dipartimento di Fisica 'E.R. Caianiello' dell'Università and Gruppo Collegato INFN, Salerno, Italy*
[32] *Dipartimento di Scienze e Innovazione Tecnologica dell'Università del Piemonte Orientale and Gruppo Collegato INFN, Alessandria, Italy*
[33] *Dipartimento Interateneo di Fisica 'M. Merlin' and Sezione INFN, Bari, Italy*
[34] *Division of Experimental High Energy Physics, University of Lund, Lund, Sweden*
[35] *Eberhard Karls Universität Tübingen, Tübingen, Germany*
[36] *European Organization for Nuclear Research (CERN), Geneva, Switzerland*
[37] *Excellence Cluster Universe, Technische Universität München, Munich, Germany*
[38] *Faculty of Engineering, Bergen University College, Bergen, Norway*
[39] *Faculty of Mathematics, Physics and Informatics, Comenius University, Bratislava, Slovakia*
[40] *Faculty of Nuclear Sciences and Physical Engineering, Czech Technical University in Prague, Prague, Czech Republic*
[41] *Faculty of Science, P.J. Šafárik University, Košice, Slovakia*
[42] *Faculty of Technology, Buskerud and Vestfold University College, Vestfold, Norway*
[43] *Frankfurt Institute for Advanced Studies, Johann Wolfgang Goethe-Universität Frankfurt, Frankfurt, Germany*
[44] *Gangneung-Wonju National University, Gangneung, South Korea*
[45] *Gauhati University, Department of Physics, Guwahati, India*
[46] *Helsinki Institute of Physics (HIP), Helsinki, Finland*
[47] *Hiroshima University, Hiroshima, Japan*
[48] *Indian Institute of Technology Bombay (IIT), Mumbai, India*
[49] *Indian Institute of Technology Indore, Indore (IITI), India*
[50] *Inha University, Incheon, South Korea*
[51] *Institut de Physique Nucléaire d'Orsay (IPNO), Université Paris-Sud, CNRS-IN2P3, Orsay, France*
[52] *Institut für Informatik, Johann Wolfgang Goethe-Universität Frankfurt, Frankfurt, Germany*
[53] *Institut für Kernphysik, Johann Wolfgang Goethe-Universität Frankfurt, Frankfurt, Germany*
[54] *Institut für Kernphysik, Westfälische Wilhelms-Universität Münster, Münster, Germany*
[55] *Institut Pluridisciplinaire Hubert Curien (IPHC), Université de Strasbourg, CNRS-IN2P3, Strasbourg, France*
[56] *Institute for Nuclear Research, Academy of Sciences, Moscow, Russia*
[57] *Institute for Subatomic Physics of Utrecht University, Utrecht, Netherlands*
[58] *Institute for Theoretical and Experimental Physics, Moscow, Russia*
[59] *Institute of Experimental Physics, Slovak Academy of Sciences, Košice, Slovakia*
[60] *Institute of Physics, Academy of Sciences of the Czech Republic, Prague, Czech Republic*
[61] *Institute of Physics, Bhubaneswar, India*
[62] *Institute of Space Science (ISS), Bucharest, Romania*

JHEP03(2016)082

[63] Instituto de Ciencias Nucleares, Universidad Nacional Autónoma de México, Mexico City, Mexico
[64] Instituto de Física, Universidad Nacional Autónoma de México, Mexico City, Mexico
[65] iThemba LABS, National Research Foundation, Somerset West, South Africa
[66] Joint Institute for Nuclear Research (JINR), Dubna, Russia
[67] Konkuk University, Seoul, South Korea
[68] Korea Institute of Science and Technology Information, Daejeon, South Korea
[69] KTO Karatay University, Konya, Turkey
[70] Laboratoire de Physique Corpusculaire (LPC), Clermont Université, Université Blaise Pascal, CNRS-IN2P3, Clermont-Ferrand, France
[71] Laboratoire de Physique Subatomique et de Cosmologie, Université Grenoble-Alpes, CNRS-IN2P3, Grenoble, France
[72] Laboratori Nazionali di Frascati, INFN, Frascati, Italy
[73] Laboratori Nazionali di Legnaro, INFN, Legnaro, Italy
[74] Lawrence Berkeley National Laboratory, Berkeley, California, United States
[75] Moscow Engineering Physics Institute, Moscow, Russia
[76] Nagasaki Institute of Applied Science, Nagasaki, Japan
[77] National Centre for Nuclear Studies, Warsaw, Poland
[78] National Institute for Physics and Nuclear Engineering, Bucharest, Romania
[79] National Institute of Science Education and Research, Bhubaneswar, India
[80] Niels Bohr Institute, University of Copenhagen, Copenhagen, Denmark
[81] Nikhef, Nationaal instituut voor subatomaire fysica, Amsterdam, Netherlands
[82] Nuclear Physics Group, STFC Daresbury Laboratory, Daresbury, United Kingdom
[83] Nuclear Physics Institute, Academy of Sciences of the Czech Republic, Řež u Prahy, Czech Republic
[84] Oak Ridge National Laboratory, Oak Ridge, Tennessee, United States
[85] Petersburg Nuclear Physics Institute, Gatchina, Russia
[86] Physics Department, Creighton University, Omaha, Nebraska, United States
[87] Physics Department, Panjab University, Chandigarh, India
[88] Physics Department, University of Athens, Athens, Greece
[89] Physics Department, University of Cape Town, Cape Town, South Africa
[90] Physics Department, University of Jammu, Jammu, India
[91] Physics Department, University of Rajasthan, Jaipur, India
[92] Physik Department, Technische Universität München, Munich, Germany
[93] Physikalisches Institut, Ruprecht-Karls-Universität Heidelberg, Heidelberg, Germany
[94] Purdue University, West Lafayette, Indiana, United States
[95] Pusan National University, Pusan, South Korea
[96] Research Division and ExtreMe Matter Institute EMMI, GSI Helmholtzzentrum für Schwerionenforschung, Darmstadt, Germany
[97] Rudjer Bošković Institute, Zagreb, Croatia
[98] Russian Federal Nuclear Center (VNIIEF), Sarov, Russia
[99] Russian Research Centre Kurchatov Institute, Moscow, Russia
[100] Saha Institute of Nuclear Physics, Kolkata, India
[101] School of Physics and Astronomy, University of Birmingham, Birmingham, United Kingdom
[102] Sección Física, Departamento de Ciencias, Pontificia Universidad Católica del Perú, Lima, Peru
[103] Sezione INFN, Bari, Italy
[104] Sezione INFN, Bologna, Italy
[105] Sezione INFN, Cagliari, Italy
[106] Sezione INFN, Catania, Italy
[107] Sezione INFN, Padova, Italy
[108] Sezione INFN, Rome, Italy
[109] Sezione INFN, Trieste, Italy
[110] Sezione INFN, Turin, Italy
[111] SSC IHEP of NRC Kurchatov institute, Protvino, Russia
[112] Stefan Meyer Institut für Subatomare Physik (SMI), Vienna, Austria

JHEP03(2016)082

[113] *SUBATECH, Ecole des Mines de Nantes, Université de Nantes, CNRS-IN2P3, Nantes, France*
[114] *Suranaree University of Technology, Nakhon Ratchasima, Thailand*
[115] *Technical University of Košice, Košice, Slovakia*
[116] *Technical University of Split FESB, Split, Croatia*
[117] *The Henryk Niewodniczanski Institute of Nuclear Physics, Polish Academy of Sciences, Cracow, Poland*
[118] *The University of Texas at Austin, Physics Department, Austin, Texas, U.S.A.*
[119] *Universidad Autónoma de Sinaloa, Culiacán, Mexico*
[120] *Universidade de São Paulo (USP), São Paulo, Brazil*
[121] *Universidade Estadual de Campinas (UNICAMP), Campinas, Brazil*
[122] *University of Houston, Houston, Texas, United States*
[123] *University of Jyväskylä, Jyväskylä, Finland*
[124] *University of Liverpool, Liverpool, United Kingdom*
[125] *University of Tennessee, Knoxville, Tennessee, United States*
[126] *University of the Witwatersrand, Johannesburg, South Africa*
[127] *University of Tokyo, Tokyo, Japan*
[128] *University of Tsukuba, Tsukuba, Japan*
[129] *University of Zagreb, Zagreb, Croatia*
[130] *Université de Lyon, Université Lyon 1, CNRS/IN2P3, IPN-Lyon, Villeurbanne, France*
[131] *V. Fock Institute for Physics, St. Petersburg State University, St. Petersburg, Russia*
[132] *Variable Energy Cyclotron Centre, Kolkata, India*
[133] *Warsaw University of Technology, Warsaw, Poland*
[134] *Wayne State University, Detroit, Michigan, United States*
[135] *Wigner Research Centre for Physics, Hungarian Academy of Sciences, Budapest, Hungary*
[136] *Yale University, New Haven, Connecticut, United States*
[137] *Yonsei University, Seoul, South Korea*
[138] *Zentrum für Technologietransfer und Telekommunikation (ZTT), Fachhochschule Worms, Worms, Germany*

JHEP03(2016)082